Factors Governing the Foldability of Proteins

D.K.Klimov and D.Thirumalai

Institute for Physical Science and Technology and Department of Chemistry and Biochemistry

University of Maryland, College Park, Maryland 20742

phone (301) 405-4803

fax (301) 314-9404

Abstract

We use a three dimensional lattice model of proteins to investigate systematically the global properties of the polypeptide chains that determine the folding to the native conformation starting from an ensemble of denatured conformations. In the coarse grained description, the polypeptide chain is modeled as a heteropolymer consisting of N beads confined to the vertices of a simple cubic lattice. The interactions between the beads are taken from a random Gaussian distribution of energies, with a mean value B_0, that corresponds to the overall average hydrophobic interaction energy. We studied 56 sequences all with a unique ground state (native conformation) covering two values of N (15 and 27) and two values of B_0. The smaller value of B_0 was chosen so that the average fraction of hydrophobic residues corresponds to that found in natural proteins. The higher value of B_0 was selected with the expectation that only the fully compact conformations would contribute to the thermodynamic behavior. For $N = 15$ the entire conformation space (compact as well as noncompact structures) can be exhaustively enumerated so that the thermodynamic properties can be exactly computed at all temperatures. The thermodynamic properties for the 27-mer chain were calculated

using slow cooling technique together with standard Monte Carlo simulations. The kinetics of approach to the native state for all the sequences was obtained using Monte Carlo simulations. For all sequences we find that there are two intrinsic characteristic temperatures, namely, T_θ and T_f. At the temperature T_θ the polypeptide chain makes a transition to a collapsed structure while at T_f the chain undergoes a transition to the native conformation. We show that foldability of sequences can be characterized entirely in terms of these two temperatures. It is shown that fast folding sequences have small values of $\sigma = (T_\theta - T_f)/T_\theta$, whereas slow folders have larger values of σ (the range of σ is $0 < \sigma < 1$). The calculated values of the folding times correlate extremely well with σ. An increase in σ from 0.1 to 0.7 can result in an increase of 5-6 orders of magnitudes in folding times. In contrast, we demonstrate that there is no useful correlation between folding times and the energy gap between the native conformation and the first excited state at any N for any value of B_0. In particular, in the parameter space of the model, many sequences with varying energy gaps all with roughly the same folding time can be easily engineered. Folding sequences in this model, therefore, can be classified based solely on the value of σ. Fast folders have small values of σ (typically less than about 0.1), moderate folders have values of σ in the approximate range between 0.1 and 0.6, while for slow folders σ exceeds 0.6. The precise boundary between these categories depends crucially on N. The range of σ for fast folders decreases with the length of the chain. At temperatures close to T_f fast folders reach the native conformation via a topology inducing nucleation collapse mechanism without forming any detectable intermediates, whereas only a fraction of molecules $\Phi(T)$ reaches the native conformation by this process for moderate folders. The remaining fraction reaches the native state via three stage multipathway process. For slow folders $\Phi(T)$ is close to zero at all temperatures. The simultaneous requirement of native state sta-

bility and kinetic accessibility can be achieved at high enough temperatures for those sequences with small values of σ. The utility of these results for *de novo* design of proteins is briefly discussed.

Keywords: protein folding; lattice Monte Carlo simulations; kinetic accessibility and stability; kinetic partitioning mechanism; topology inducing nucleation collapse.

I. INTRODUCTION

The mechanisms, by which proteins adopt well-defined three dimensional topological structures, have been extensively investigated theoretically [1–6] as well as experimentally [7,8]. The major intellectual impetus for these studies originate in the so called Levinthal paradox [9]. Since the number of conformations of even relatively short proteins is astronomically large Levinthal suggested that it would be impossible for proteins to reach the native conformation by a random search through all the available conformation space. In the last few years several groups [1–5] have provided, largely complimentary, possible theoretical resolutions to the Levinthal paradox. The unifying theme that emerges from these studies, all of which are based on certain minimal model representations of proteins [10–16,18–27] is that due to certain intrinsic preference for native structures proteins efficiently explore the underlying rough energy landscape. Explicit computations of the energy landscape for certain lattice models [28] reveal that foldable sequences (those that reach the native conformations on a relatively fast time scales, which for real proteins is typically of the order of a second) have relatively small free energy barriers. These and related studies [12,19,29] have emphasized the importance of the connectivity between various low energy states in determining the kinetic foldability of proteins. Thus, it appears that in order to fully elucidate the folding kinetics of proteins it is necessary to understand not only the low energy spectrum, but also how the various states are connected.

It is of interest to wonder if natural proteins have been designed so that the requirements of kinetic foldability and stability have been simultaneously satisfied and if so how are they

encoded in the primary sequence. If this is the case, then it follows that because protein folding is a self-assembly process the kinetic foldability of proteins should be described in terms of the properties of the sequence itself. This argument would indicate that certain intrinsic thermodynamic characteristics associated with the sequence may well determine the overall kinetic accessibility of the native conformation. The minimal models are particularly suitable for addressing this question. For these models the folding kinetic rates for every sequence can be precisely calculated for small enough values of N - the number of beads in the model polypeptide chain. In addition the energy spectrum for small values of N can be explicitly enumerated for lattice models and for moderate sized proteins it can be computed by simulation methods. Thus, these models afford a systematic investigation of the factors governing folding rates.

It is perhaps useful right at the outset to say a few words about the lattice representation of polypeptide chains. The energies employed in the minimal models (or in other knowledge based schemes) should be thought of as estimates of potentials of mean force after other irrelevant degrees of freedom are integrated out. In principle, this leaves one with an effective potential surface involving only the protein coordinates. In the minimal models one further coarse grains this force field by eliminating all coordinates except, perhaps, those associated with centers of the residues. The lattice models further confine these centers to the vertices of a chosen lattice. These arguments show that we can at best expect only qualitative themes to emerge from these studies. Nevertheless, these simulations together with other theoretical ideas have provided testable predictions for the kinetics of refolding of proteins.

By using the random energy model (REM), originally introduced as the simplest mean field spin glass model [30], as a caricature of proteins it has been proposed that the dual requirement (kinetic accessibility of the native conformation as well as the stability) can be satisfied if the ratio of the folding transition temperature T_f to an equilibrium glass transition temperature $T_{g,eq}$, at which the entropy vanishes in REM, is maximized [1,31]. (It has been noted that in order to use this criterion in lattice models $T_{g,eq}$ has to be replaced by a kinetic glass transition temperature $T_{g,kin}$ [32]. It would be desirable to clarify the

relationship between $T_{g,eq}$ and $T_{g,kin}$).

Based partially on lattice simulations of proteins a plausible relationship between folding rates and the ratio of T_f to the collapse transition temperature T_θ was conjectured a couple of years ago. In particular, Camacho and Thirumalai have argued that the fast folding sequences have small values of $\sigma = (T_\theta - T_f)/T_\theta$ [33]. The theoretical reason for such an expectation has been given recently [34]. The advantage of the criterion, based on the smallness of σ to classify fast and slow folding sequences, is that both T_θ and T_f are readily calculable from equilibrium properties. More importantly, one can deduce T_θ and T_f directly from experiments.

More recently, Sali *et al.* [20,21] have forcefully asserted that for the class of minimal models of the sort described here the necessary and sufficient condition for folding (within a preset time scale in Monte Carlo simulations) is that the native conformation be separated from the first excited state by a large gap (which is presumably measured in the units of k_BT with k_B being the Boltzmann constant and T the temperature). However, their studies are incomplete and rest on untested assumptions. They restricted their conformation space to only a search among all compact structures of a 27-bead heteropolymer. More importantly, they did not provide for their model the dependence of the folding times as a function of the gap to establish the kinetic foldability of any sequence. Thus there is no direct evidence of the dependence of the folding times for various sequences and the gap $\Delta = E_1 - E_0$ - which in the original study has been stated as a mathematical theorem. Notice that this gap has been defined as the difference between the two lowest energy levels assuming that both these correspond to compact conformations. It is, in fact, relatively straightforward to provide counter examples to this criterion [28] casting serious doubts on the general validity of the strict relationship between gap and folding times. Moreover, it is extremely difficult, if not impossible, to obtain the value of the gap for proteins either experimentally or theoretically. Thus, the practical utility of this criterion for models other than lattice systems is limited at best.

The major purpose of this study is to critically examine the various properties of se-

quences (all of which have a unique ground state) that determine the kinetic accessibility and stability of lattice representations of proteins. This is done by calculating the folding rates and thermodynamic properties using $N = 15$ for a number of sequences. The qualitative lesson from this case is verified by studying a smaller number of sequences for the much studied case of $N = 27$. The rest of the paper is organized as follows: In Sec. (II) the complete details of the model as well as simulation methods are discussed. The results of this study for a variety of cases are given in Sec. (III). The paper is concluded in Sec. (IV) with a discussion.

II. DESCRIPTION OF THE MODEL AND SIMULATION TECHNIQUES

A. Model

We model proteins as chains of N successively connected beads (residues) located at the sites of an infinite cubic lattice (Figs. (1,2)). To satisfy self-avoiding condition we impose the restriction that each lattice site can be occupied only once (or remain free). The length of the bond between two residues is fixed and is equal to the lattice spacing $a = 1$. Any conformation (structure, in lattice terms), which the protein can adopt, is described by $\mathbf{r}_i$ $(i = 1, .., N)$ vectors with discrete coordinates $x_i, y_i, z_i = 0, 1, 2...$, which are the positions of residues on the lattice. We assume that the only interactions, contributing to the total energy of a protein structure, are those that arise due to the interactions between residues that are far apart along a chain. We further assume that the interactions are short ranged and can be represented by topological contacts between residues. A topological contact is formed when two nonbonded beads i and j ($\mid i - j \mid \geq 3$) are nearest-neighbors on the cubic lattice, i.e., $\mid \mathbf{r}_i - \mathbf{r}_j \mid = a$. Thus, the total energy of a protein E is given by the sum of the energies assigned to topological contacts found in a structure, i.e

$$E = \sum_{i<j+3} B_{ij}\delta(r_{ij} - a), \tag{1}$$

where B_{ij} is the interaction energy between ith and jth residues, which form a topological contact, $r_{ij} =\mid \mathbf{r}_i - \mathbf{r}_j \mid$ is the distance between them, and $\delta(0) = 1$ and 0 otherwise. In order to take into account the heterogeneity of interactions found in real proteins we assume that the interaction energies B_{ij} have a Gaussian distribution of the form [20–23]

$$P(B_{ij}) = \frac{1}{(2\pi B^2)^{1/2}} \exp\Big(-\frac{(B_{ij} - B_0)^2}{2B^2}\Big), \tag{2}$$

where B_0 is the mean value and B is the standard deviation. This model that has been extensively investigated theoretically [20,21,23,35]. It should be stressed that the models studied here and similar lattice models are at best caricatures of real proteins [36]. The only objective of these studies should be to obtain qualitative behavior which hopefully shed light on the experiments. This, of course, requires extrapolating from these model systems to the behavior expected in proteins in terms of experimentally variable parameters. A tentative proposal for achieving this has recently been given [34].

B. Choice of B_0

Since the actual energy scales are not known, we set B in Eq. (2) equal to 1 and thus all energies are expressed in the units of B. In contrast, we will demonstrate that the precise value of B_0 (or more precisely the ratio B_0/B) plays a crucial role. Negative values of B_0 favor random collapse of the chain as the temperature is lowered. In addition, the mean value B_0 controls the nature of conformations that constitute the low energy part of the spectrum. The extensive full enumeration study of the conformational space for different sequences of various lengths N indicates that as the mean value B_0 decreases structures with maximum number of topological contacts (compact structures, CS) start to dominate among conformations with minimum energies [21,37]. Furthermore, a relationship can be obtained between the value of B_0 and the ratio of hydrophilic and hydrophobic residues in a sequence. This would be relatively straightforward for random site models of the sort introduced recently [38]. For the random bond case, that is the subject of this

and numerous previous studies, the computation of the fraction of hydrophobic residues is somewhat ambiguous. Nevertheless, the following procedure can be used to calculate their fraction. Since it is natural to identify negative interaction energies as those between hydrophobic residues and positive ones to be between hydrophilic residues, one can specify boundary energies B_H and B_P ($B_H = -B_P$) in such a way that the energies B_{ij} below B_H corresponds to hydrophobic interactions and the energies above B_P pertain to hydrophilic interactions. The energies B_{ij}, lying between these boundaries, are associated with mixed interactions. If the number of hydrophobic and hydrophilic residues in a sequences is N_H and N_P, respectively, ($N_H + N_P = N$), the fraction of hydrophobic energies λ_H among B_{ij} is roughly $(N_H/N)^2$. This fraction can be also obtained by integrating the distribution (2) from infinity to the energy B_H. The relationship between λ_H and B_0 may be obtained as

$$\lambda_H \simeq (N_H/N)^2 = \int_{-\infty}^{B_H} P(B_{ij}) dB_{ij}. \tag{3}$$

The precise value of B_H (and B_P) can easily be determined if one considers the case with $B_0 = 0$, for which $N_H = N_P$. Using Eqs. (2) and (3) we find that $B_H = -0.675$ (for this particular value of B_0 one quarter of all energies B_{ij} are below the boundary energy B_H and one quarter - above B_P). It is known that in natural proteins hydrophobic residues make up approximately 54 percent of all residues in a sequence [39]. For the distribution in Eq. (2) this implies that the mean value B_0 should be approximately -0.1. Most of our simulations have been performed with this value of B_0.

We have also performed a study of the sequences with $B_0 = -2.0$ that in the language of sequence composition means that hydrophobic residues constitute about 94 percent of all residues. The motivation for choosing this value of B_0 is the following. For $B_0 = -2.0$ the low energy spectrum becomes more sparse [21], because as mentioned above the main contribution comes from CS, whose total number is considerably less than the number of conformations with any other number of topological contacts c. Specifically, for $N = 15$ the number of conformations having $c = 11$ is 3,848, $c = 10$ - 17,040, $c = 9$ - 97,216, $c = 8$ - 313,868 etc. Studying the folding rates of the sequences having different B_0 enables us

to assess the role of the available conformation space and the connectivity between various states in determining the kinetics of the folding process. The choice of $B_0 = -2.0$ also allows us to compare directly our results to previous studies found in the literature [20,21].

C. Choice of N

In order to fully characterize the folding scenarios it is necessary to understand the kinetics of approach to a native conformation in these models as a function of N and temperature. It has been shown recently that the folding of real proteins depends critically on N, the characteristic temperatures of the polypeptide chain (T_θ, T_f, and perhaps the kinetic glass transition temperature T_g), viscosity, surface tension γ etc. [34]. Thus in order to make the results of the minimal models relevant to proteins it is imperative to vary N in the simulations.

Although one would like to understand the kinetic behavior of foldable heteropolymers for sufficiently large N this is currently computationally difficult. In the present study we have chosen $N = 15$ and $N = 27$. We chose $N = 15$ because for this value one can perform detailed kinetic study by including *all conformations* (compact and noncompact). A detailed study for three dimensional (3D) lattice models comparable to that undertaken for two dimensional (2D) systems has never been done [2,12,13,40]. With this value of N one of the limitations of the study of Sali *et al.*, who restricted themselves to compact structures only, can be overcome. From any theoretical perspective the qualitative difference in results between $N = 15$ and $N = 27$ should be insignificant. This is certainly the experience in simulations of polymeric systems [40]. Thus, we expect that the qualitative aspects of the kinetics of folding should be quite similar for $N = 15$ and 27. This is, in fact, the case.

One might naively think that for $N = 15$ the total number of conformations is not enough for folding times to exceed the Levinthal time, which is roughly the number of conformations of the polypeptide chain. The basis for this argument is that the conformation space of $N = 15$ is considerably less than for $N = 27$. The total number of conformations of the

chain of N residues C_N or equivalently the number of all possible self-avoiding walks of $N-1$ steps on a cubic lattice is [41]

$$C_N \approx a(N-1)^{\gamma-1} Z_{\rm eff}^{N-1} \tag{4}$$

where $Z_{\rm eff} = 4.684$, the universal exponent $\gamma \approx 1.16$, and $a = o(1)$. For $N = 15$ and 27 C_N is approximately 7.77×10^8 and 4.6×10^{17}, respectively. Full enumeration (FE) of SAW which are *unrelated* by symmetry for $N = 15$ gives $C_{15}^{FE} = 93,250,730$, which differs approximately from the number of *all* SAW by a factor of 48. Thus, C_{15} obtained from Eq. (4) and C_{15}^{FE} are consistent. The chain of 15 residues can form 3,848 CS, which belong to 3x3x2 or 4x2x2 tetragonals, whereas 27-mer chain adopts 103,346 CS with 28 topological contacts [35,41]; all these CS are confined to 3x3x3 cube.

From the above enumerations of the conformations it might be tempting to speculate that virtually all sequences for $N = 15$ with a unique ground state should fold on the Levinthal time scale of 9.3×10^7 Monte Carlo steps (MCS). However, we find that for some of the thirty two sequences examined the maximum folding time can be larger than 10^9 MCS depending upon several characteristics (see below). Thus, even if the chain samples one conformation per MCS the bottlenecks in the energy surface can prevent the chain from reaching the native conformation. This implies that the number of conformations alone cannot determine folding times [29]. In fact, in the case of the models of disulfide bonded proteins it has been explicitly demonstrated that a significant reduction of available conformation space does not guarantee a decrease in folding times [28]. Thus, kinetic foldability is determined by several factors and hence explicit studies of $N = 15$, where full enumeration of all conformations is possible, should help us gain insights into the folding of small proteins. A comparison of the results for small values of N is also useful in assessing finite size effects.

The arguments given above together with explicit computations given here reject claims [42] that the study of short chains ($N < 27$ in three or two dimensions) are not of significance in illustrating the qualitative behavior of protein folding kinetics. Numerous studies have shown that it is not merely the size of the conformation space, but the connectivity

between conformations, i.e. the nature of the underlying energy landscape that allows one to distinguish between foldable and non-foldable sequences [29]. The obvious advantage of $N = 15$ is that systematic thermodynamic and kinetic studies (already performed for 2D chains of N up to 30) can be undertaken for 3D chains.

D. Correlation Functions

For probing the thermodynamics and kinetics of protein folding we use the overlap function (considered here as an order parameter), which is defined as [33]

$$\chi = 1 - \frac{1}{N^2 - 3N + 2} \sum_{i \neq j, j \pm 1} \delta(r_{ij} - r_{ij}^N), \tag{5}$$

where r_{ij}^N refers to the coordinates of the native state. This function measures structural similarity between the native state and the state of interest: the smaller the value of χ becomes the larger a given structure resembles the native one. Additional structural and kinetic information can be obtained using the function Q, which counts the relative number of native-like topological contacts in a structure [11,20,21,24]

$$Q = \frac{c_n}{c_n^{tot}}, \tag{6}$$

where c_n is the number of native-like contacts in a given structure and c_n^{tot} is the total number of contacts found in the native structure.

We have calculated the relevant thermodynamic properties such as the total energy $< E >$, the specific heat C_v with

$$C_v = \frac{< E^2 > - < E >^2}{T^2}, \tag{7}$$

the function $< Q >$, and the Boltzmann probability of being in the native state

$$P(E_0) = \frac{\exp(-\beta E_0)}{Z}, \tag{8}$$

where $Z = \sum_i \exp(-\beta E_i)$ and $\beta = 1/(k_B T)$ (k_B is set to 1 in our simulations). The brackets $< ... >$ indicate the thermodynamic averages. In addition, the overlap function and the fluctuations in $< \chi >$, namely

$$\Delta\chi = < \chi^2 > - < \chi >^2 \tag{9}$$

were also calculated. The thermodynamic characteristics of the system can be exactly calculated for each sequence by exhaustively enumerating the various symmetry unrelated conformations for small enough values of N. In particular, we calculated these quantities exactly for $N = 15$. For $N = 27$ we used slow cooling Monte Carlo method to calculate the appropriate quantities of interest. The annealing simulation procedure is discussed in Appendix A.

The parameter that distinguishes fast folding and slow folding sequences appears to be $\sigma = (T_\theta - T_f)/T_\theta$, where T_θ is the collapse transition temperature and T_f is the folding transition temperature [33,34]. It is known that even in these finite sized systems T_θ can be estimated using the peak in the temperature dependence of C_v (cf. Eq. (7)) [25,33,43]. We have shown in previous studies involving both lattice and off-lattice models that the temperature dependence of the fluctuations in the overlap function, which serves as an order parameter, can be used to calculate T_f [33,44]. In particular, T_f corresponds to the peak in the function $\Delta\chi$.

For most sequences T_θ and T_f are sufficiently well separated that an unambiguous determination is possible by a straightforward computation of the temperature dependence of C_v and $\Delta\chi$. However, we have generated five sequences (out of 32 for $N = 15, B_0 = -0.1$), for which C_v or $\Delta\chi$ appear not to have well-defined single maximum due to specific arrangement of the energy states. For example, sequence 32 shows two maxima in the dependence $C_v(T)$ at $T_1 = 0.28$ and $T_2 = 0.73$ of different amplitudes $C_v(T_1) = 8.25$ and $C_v(T_2) = 13.22$, respectively. In this case, we defined T_θ as a weighted average over the temperatures T_1 and T_2

$$T_\theta = \frac{C_v(T_1)T_1 + C_v(T_2)T_2}{C_v(T_1) + C_v(T_2)}. \tag{10}$$

In other instances (e.g., for sequence 10), we found that although the dependence $C_v(T)$ has a single maximum at T_{max}, it also has the interval (T', T'') not including T_{max}, wherein the derivative $\frac{dC_v}{dT}$ again approaches almost zero value that gives essentially unsymmetric

form to the peak of specific heat. We have also applied Eq. (10) for calculating T_θ for such sequences by setting $T_1 = T_{max}$ and $T_2 \neq T_{max}$ corresponds to the temperature, at which $|\frac{dC_v}{dT}|$ has the smallest value within (T', T'').

There are other ways of calculating T_θ and T_f. For example, T_θ could be directly inferred from the temperature dependence of the radius of gyration of the polypeptide chain. It has been shown in our earlier work on off-lattice models [43] that the resulting values of T_θ coincide with those obtained from the peak in the specific heat. The folding transition temperature is often associated with the midpoint of the temperature dependence of the probability of being in the native conformation. This estimate of T_f is in good agreement with the peak position of the temperature dependence of $\Delta\chi$. In general, different order parameters can be used to calculate T_f. The resulting values are fairly consistent with each other.

E. Sequence Design

To create a database of different sequences for $N = 15$ we generated 60 random sequences, using the mean value $B_0 = -0.1$ and 9 random sequences, using $B_0 = -2.0$. For $N = 27$ we generated 15 random sequences with $B_0 = -0.1$ and 2 with $B_0 = -2.0$. Note that the computational procedures for 15-mer and 27-mer sequences are similar, except that thermodynamic quantities for $N = 27$ are calculated from slow cooling Monte Carlo simulations. By enumerating all possible conformations for $N = 15$ we determined the energy spectrum for each sequence. The program for enumerating all the structures a protein can adopt on a cubic lattice is based on the Martin algorithm [45] that is supplemented by the procedure that rejects all structures related by symmetry. This algorithm allows us to determine the lowest (native) energy state E_0, its degeneracy g, the coordinates of corresponding structure(s), and the number of topological contacts c for each sequence. The energy levels for 10 sequences are summarized in Fig. (3) for $N = 15, B_0 = -0.1$ and in Fig. (4) for $N = 27, B_0 = -0.1$. The spectra for $N = 15$ were obtained by enumerating

all possible conformations of the chain and arranging them in increasing order of energy. For $N = 27$, on the other hand, the spectra for the various sequences are obtained by slow cooling Monte Carlo method, the details of which are reported in Appendix B. The results in Fig. (4) for $N = 27$ are instructive. For each sequence we show two columns. The left column gives the spectrum calculated by numerical method, whereas the right column is the spectrum that would be obtained if only the compact structures were retained. A comparison of the two columns for various sequences clearly reveals that for a majority of sequences the low lying energy levels are, in fact, noncompact. Thus, from this figure we would conclude that these noncompact structures would make significant contributions to various thermodynamic properties. This figure also shows that for the sequences whose native conformation is compact, the energy gap Δ_{CS} calculated using compact structures spectrum alone exceeds the true gap. This appears to be a general result and can be understood by noting that the lowest energy excitations for such sequences are created by flipping surface bonds. The resulting structure would be noncompact and its energy would be lower or equal to that of other compact structures. Thus, it should in general be true that when the native conformation is compact, $\Delta_{CS} \geq \Delta$. Since there are large scale motions that are expected to be involved in protein folding the physically relevant energy scale should be the stability gap [16,17]. There is no straightforward relationship between the stability gap and Δ_{CS} or Δ. We rejected all sequences with nonunique ground state from further analysis.

In order to determine folding times for a range of σ $(= (T_\theta - T_f)/T_\theta)$ values sequences with varying spectral characteristics are required. It is known that a generic randomly generated sequence (even with unique native state) does not fold rapidly [1,2,4]. Thus, to expand the database of the sequences we used a technique proposed by Shakhnovich and Gutin [46,47] to create a set of optimized sequences. We should stress that in our study this was used as merely a technical device to generate sequences that span a rather wide range of σ. Here we will briefly present the idea of this scheme [46,47]. One selects an arbitrary ('target') structure corresponding to a given initial random sequence. Then standard Monte Carlo

algorithm is applied in the sequence space. The first step of this scheme can be described in the following way. Two energies B_{ij} and B_{kl} of the initial ('old') sequence picked at random are interchanged, so that the topological contact between residues k,l has the interaction energy $B'_{kl} = B_{ij}$ and the contact between residues i,j - the interaction energy $B'_{ij} = B_{kl}$. Thus, a new probe sequence, which differs from the initial one by the energies B'_{ij} and B'_{kl}, is produced and is subject to Metropolis criterion. To do this, the energy of the new sequence E_{new} fitted to the target structure is calculated and compared with E_{old} of the initial sequence. If the new sequence provides lower energy at the target structure, it is unconditionally accepted and $B_{ij} = B'_{ij}$, $B_{kl} = B'_{kl}$. If $E_{old} < E_{new}$, the new sequence is accepted with the Boltzmann probability $P = \exp(-(E_{new} - E_{old})/T)$. If the new sequence is rejected, the initial sequence is restored. This permutation procedure, which does not alter the composition of the sequences, is repeated n times. The control parameter is temperature, and if it is sufficiently low, a series of sequences are quickly generated after relatively small number of MCS (10^4), whose energies when fitted to the target structure are remarkably low. By employing the full enumeration procedure (or Monte Carlo simulations for $N = 27$) one can verify that these energies are actually the lowest ones in the spectrum. In this manner, a series of new 'optimized' sequences are created. An application of optimization scheme allowed us to investigate essentially wider range of values of the parameter σ than can be done by analyzing sequences produced at random.

In all, for $N = 15$ we chose 32 sequences with $B_0 = -0.1$ and 9 sequences with $B_0 = -2.0$ for detailed study. Among these with $B_0 = -0.1$, 15 sequences were random and 17 - optimized. The native structures of these sequences were CS (e.g., structure (a) in Fig. (1)) as well non-CS (e.g., structure (b)) and included from 8 to 11 topological contacts. For $B_0 = -2.0$ all sequences were optimized and as suspected the native conformations were all CS [21]. For $N = 27$ we analyzed 15 optimized sequences with $B_0 = -0.1$ and 2 with $B_0 = -2.0$. As for $N = 15$ their native conformations were CS as well as non-CS with 21-28 topological contacts (Fig. (2)). We believe that this choice of sequences is sufficient and we do not expect qualitatively different behavior for this model, if a larger database is selected.

Since our objective is to compare the rates of folding for different sequences it is desirable to subject them to identical folding conditions. The equilibrium value of $< \chi >$ measures the extent to which the conformation at a given temperature is exactly equivalent to a microscopic conformation, namely the native state. At sufficiently low temperature $< \chi >$ would approach zero, but the folding time may be far too long. We chose to run our Monte Carlo simulations at a sequence dependent simulation temperature T_s that is subject to two conditions: (a) T_s be less than T_f for a specified sequence so that the native conformation has the highest occupation probability; (b) the value of $< \chi(T = T_s) >$ be a constant for all sequences, i.e.

$$< \chi(T = T_s) >= \alpha. \tag{11}$$

In our simulations we choose $\alpha = 0.21$ and this value was low enough so that $T_s/T_f < 1$ for all the sequences examined. This general procedure for selecting the simulation temperatures has been previously used in the literature [21,28]. For $N = 15$ T_s is precisely determined using Eq. (11) because $< \chi(T = T_s) >$ can be calculated exactly using the full enumeration procedure. The simulation temperatures for $N = 27$ are calculated using the protocol described in Appendix A.

F. Monte Carlo Simulations and Interpretation of Folding Kinetics

In the present work we used standard Monte Carlo (MC) algorithm for studying folding of different sequences to their native states. The local simulation dynamics includes the following moves (Fig. (5)): (i) corner moves, which flip the position of jth residue across the diagonal of the square formed by bonds $(j-1, j)$ and $(j, j+1)$; (ii) crankshaft rotations, which involve changing the positions of two successively connected beads $j + 1$ and $j + 2$ (positions of j and $j+1$ beads, which are nearest neighbors on a lattice, remain unchanged); (iii) rotations of end beads, in which the end bead (1 or N) moves to any of 5 adjacent sites to the beads 2 or $N-1$ (the sites previously occupied by the beads 1 or N are not considered

as possible new sites). This particular set of moves has already been applied in Monte Carlo simulations [21,32]; for a discussion of the dependence of the kinetic results on the move set used in the Monte Carlo simulations see Ref. 13. In order to ensure maximum efficiency of exploring conformation space it is reasonable to assign different probabilities for the moves (i), (iii) and the move (ii). After probing several values we found that the probability $p = 0.2$ for the moves (i) and (iii) (involving single residue) provides the best efficiency of searching a native state of a test sequence by Monte Carlo algorithm. Qualitatively, it is clear that very small probability of moves (ii) depletes the ability of a chain to sample different conformations, while excessively high probability of their occurrence may deteriorate the ability to accept moves that would lead to acquisition of the last few native contacts when the chain is near the native conformation.

For clarity of presentation let us now describe one step of the Monte Carlo algorithm. In the beginning, the type of move (single bead move ((i) or (iii)) or crankshaft rotation (ii)) is selected at random taking into account the probability p introduced above. After this a bead in the chain is chosen at random and the possibility of performing the selected move depending on the local configuration of the chain is established as follows. If there is a chain turn at the bead j selected for move (i) or in the case of move (ii) the beads $j, j+3$ are lattice nearest neighbors, a move is accomplished; otherwise, one must return to selection of move type. Then a self-avoidance criterion is applied: if the move results in double occupancy of lattice sites, it is rejected and a new selection of move type has to be made. If self-avoidance criterion is satisfied, the new conformation is adopted and Metropolis criterion is used, i.e., the energies of old and new conformations, E_{old}, E_{new}, are compared. If new conformation has lower energy, the move is accepted and a Monte Carlo step is completed. If E_{new} is higher than E_{old}, then the Boltzmann probability $P = \exp(-(E_{new} - E_{old})/T)$ is calculated and compared with a random number ξ $(0 < \xi < 1)$. If ξ is smaller than P, the move is accepted and MC step is completed. Otherwise, the move is rejected and the previous MC step is counted as a new one. The fraction of accepted steps on average constitutes 5-15 percents for the entire trajectory. In principle, using ergodic measures this percentage can

be adjusted *a priori* to maximize sampling rate [48].

The initial conformations of all trajectories correspond to random extended coil ('infinite temperature' conformation). After a sudden temperature quench the chain dynamics was monitored for approximately 10^5 to 5 x 10^7 MC steps (MCS), depending on a folding kinetics of a given sequence. In order to obtain the kinetics of folding for a particular sequence the dynamics was averaged over M independent initial conditions. For example, $< \chi(t) >$ is calculated as

$$< \chi(t) >= \frac{1}{M} \sum_{i=1}^{M} \chi_i(t), \tag{12}$$

where $\chi_i(t)$ is the value of χ for the i^{th} trajectory at time t. Another important probe of folding kinetics is the fraction of trajectories $P_u(t)$ which have not yet reached the native conformation at time t

$$P_u(t) = 1 - \int_0^t P_{fp}(s)ds, \tag{13}$$

where $P_{fp}(s)$ is the probability of the first passage to the native structure at time s defined as

$$P_{fp}(s) = \frac{1}{M} \sum_{i=1}^{M} \delta(s - \tau_{1i}) \tag{14}$$

In Eq. (14) τ_{1i} denotes the first passage time for the i^{th} trajectory. Similarly, other quantities were calculated. Typically, the number of trajectories M used in the averaging varied from 100 to 800. We find that for smaller values one cannot get reliable results at all. If M as small as 10 is used [21], one can obtain qualitatively incorrect results. The precise choice of M (which is sequence dependent) was determined by the condition that the resulting kinetic and thermodynamic properties should not change significantly with subsequent increase in M. The tolerance used in determining M was that the various quantities of interest converge to within 5 percent.

G. Computation of Folding Rates

The most important goal of this paper is to obtain folding times for sequences at various temperatures. These times (or equivalently the folding rates) were calculated by analyzing the time dependent behavior of the dynamic quantities. It is clear that $< \chi(t) >$ provides the most microscopic description of the kinetics of approach to the native state. The folding times reported here were obtained by a quantitative analysis of $< \chi(t) >$. For all sequences we find that after a transition time $< \chi(t) >$ can be fitted as a sum of exponentials, i.e.,

$$< \chi(t) >= a_1 \exp(-\frac{t}{\tau_{TINC}}) + a_2 \exp(-\frac{t}{\tau_f}) \tag{15}$$

In most cases, biexponential fit like in Eq. (15) gave the best approximation to the computed kinetic curves. However, for some sequences it was found that a single or three exponential fit were more suitable. The interpretation of the amplitudes a_1, a_2 and the time constants τ_{TINC}, τ_f are discussed in Sec. (III.A.3) . It must be noted that the kinetic curves for very slow folding sequences (those with large values of σ) do not reach the required equilibrium values. However, even in these instances (6 out of 32 for $N = 15, B_0 = -0.1$) our simulations were long enough to observe the transition to the native conformation so that an accurate estimate of the folding time can be made. It should be noted that the trends in folding times remain unchanged if the mean first passage time is substituted for τ_f (or τ_{TINC}) in Eq. (15).

H. Monitoring Intermediates in Folding Process

Since the underlying energy landscape in proteins is thought to be rugged [1,2,5] it is likely that there are low energy basins of attraction, in which the protein can get trapped in for arbitrary long times. Explicit construction of such landscape in lattice models, albeit in two dimensions, has revealed the presence of such states as important kinetic intermediates in certain folding pathways [28,33]. In our simulations we have used the following strategy to describe the nature of intermediates in the folding of the various sequences. We divided

each trajectory into two parts: the first part starts at the beginning of the trajectory ($t = 0$) and ends when the native structure is formed for the first time, i.e. when the first passage time τ_{1i} for the i^{th} trajectory is reached. We labeled the trajectory for $0 \leq t \leq \tau_{1i}$ as the relaxation part. The remaining portion of the trajectory for $\tau_{1i} \leq t \leq t_{max}$ is referred to as the fluctuation part, where t_{max} is the maximum time for which the computations are done for a given sequence. Using the trajectories corresponding to the relaxation regime we calculated for each sequence the probability of occurrence of the low energy states E_k, i.e.

$$P_r(E_k) = \frac{1}{M} \sum_{i=1}^{M} \frac{1}{\tau_{1i}} \int_{t=0}^{\tau_{1i}} \delta(E_i(t) - E_k) dt, \tag{16}$$

where $E_i(t)$ is the energy at the i^{th} trajectory at the time t. The state with the energy E_k, which has the largest value of P_r, is defined to be a kinetic intermediate for a given sequence. We also calculated the probability that this state occurs in the fluctuation parts of the trajectories. The fluctuation probability that the kinetic intermediates with the energy E_k (for conformations other than the native one there could be more than one structure with the same energy) are visited after the transition to the native conformation is defined as

$$P_{fl}(E_k) = \frac{1}{M} \sum_{i=1}^{M} \frac{1}{t_{max} - \tau_{1i}} \int_{t=\tau_{1i}}^{t_{max}} \delta(E_i(t) - E_k) dt, \tag{17}$$

where t_{max} is the maximum time of simulation. This quantity was calculated to monitor if the chain, after reaching the native conformation, makes a transition to the same intermediate which was visited with overwhelming probability on the way to the native conformation.

III. RESULTS

Since this section describes in complete detail the results for a variety of cases making it quite lengthy we provide a brief summary of its contents. The general methodology described in the previous section has been used to study in extreme detail the kinetics of folding for $N = 15$. For this value of N we have considered two values of B_0 which sets the overall strength of the hydrophobic interactions. We have chosen $B_0 = -0.1$ and $B_0 = -2.0$. The

former choice is a bit more realistic, while the latter was chosen to contrast the role of CS versus non-CS in determining the thermodynamics and kinetics of folding. As emphasized before the value of $N = 15$ is about the largest value of N for which exact enumeration studies are possible in three dimensions and for which the kinetics can be precisely determined in terms of all allowed conformations being explored. The results for $N = 15$ and for $B_0 = -0.1$ and $B_0 = -2.0$ are presented in Sec. (III.A). In Sec. (III.B) we present the results for $N = 27$, for which we have also chosen $B_0 = -0.1$. The thermodynamic properties with $B_0 = -2.0$ are discussed as well. A comparison of $N = 15$ and $N = 27$ shows very similar qualitative behavior.

A. $N = 15$: $B_0 = -0.1$ and $B_0 = -2.0$

1. Thermodynamic Characteristics

The two relevant temperatures T_θ and T_f for each sequence are computed from the temperature dependence of C_v and $\Delta\chi$, respectively. In addition we have computed $< Q >$ and $< \chi >$ as a function of temperature. The midpoints in the graphs of these quantities can sometimes be used to obtain an estimate of T_f. In general, T_f obtained from the peak of $\Delta\chi$ is smaller than that determined from the midpoint of $< \chi >$ or $< Q >$. The plots of $< \chi >$, $\Delta\chi$,$< Q >$, and C_v as a function of temperature are displayed in Fig. (6) for the sequence labeled 14. From the graphs of C_v and $\Delta\chi$ the collapse transition temperature T_θ and the folding transition temperature T_f are found to be 0.65 and 0.45 respectively. The simulation temperature, T_s, is calculated using Eq. (11) and in this case it turns out to be 0.38. In Fig. (7a) we present the dependence of T_s on the crucial parameter $\sigma = (T_\theta - T_f)/T_\theta$. In addition we also display the correlation between T_s and the energy gap Δ (Fig. (7b)). From these figures it appears that T_s correlates well with σ. Thus as far as the simulation temperature is concerned it appears that T_s is decreasing function of σ. This implies that if σ is small then the simulation temperature can be made higher and fast folding can therefore be expected.

This is further quantified in Sec. (III.A.4). We should emphasize that this correlation is only statistical in the sense that large (small) values of σ yield small (large) values of T_s. However given two values of σ that are closely spaced it is not possible to predict the precise values of T_s.

Since the dimensionless parameter σ serves to distinguish between foldable sequences and those that do not reach their native conformation on a reasonable time scale it is interesting to see if σ can correlate with the spectrum of the underlying energy function. It has been argued that the only important parameter that is both necessary and sufficient to account for foldability is the gap Δ [20,21,42]. The plot of σ as a function of Δ is shown in Fig. (8a). In the lower panel (Fig. (8b)) we plot σ as a function of the dimensionless parameter Δ/T_s. This figure shows very clearly the lack of correlation between σ and Δ. Thus, it is seen that no clear correspondence exists even in these models between σ and Δ. This, of course, is not surprising because T_θ is determined by the entire energy spectrum - most notably the higher energy non-compact structures. The results in Fig. (8a) show that large values of σ appear to correspond well with small values of Δ. On the other hand small values of σ simultaneously corresponds to both small as well as large values of Δ.

2. Contribution to Thermodynamic Properties from Non-compact Structures

The number of non-compact structures even for small values of N (such as 15 and 27) far exceeds that of compact structures. It has already been mentioned that full enumeration of all self-avoiding structures in three dimensions becomes increasingly difficult for $N > 15$. Thus in the literature it has been explicitly assumed that, in general, the native conformation in this model is maximally compact and that the thermodynamic properties can be determined using the spectrum of compact structures alone [20,21,49]. It has also been argued that the only relevant aspect of the energy spectrum that determines both kinetics and thermodynamics of folding in these models is the gap defined as

$$\Delta = E_1 - E_0, \tag{18}$$

where E_0 and E_1 are the lowest energy and the energy of the first excited state in the spectrum. Since we have enumerated all possible conformations for $N = 15$ this can be explicitly checked by comparing various thermodynamic quantities computed exactly with those obtained by including only the contribution from compact structures. This has been done for several sequences and the typical results for two sequences are shown in Figs. (9) and (10). In Fig. (9) we present the results for $< \chi >$ and $\Delta\chi$ for $B_0 = -0.1$. The relatively small but realistic value of B_0 makes the comparison between these quantities calculated using CS alone and the values calculated using full enumeration least favorable. From Fig. (9a) we find that T_s found from full enumeration is roughly one half that obtained using compact structures enumeration (CSE) alone. In fact, T_s^{CSE} exceeds the collapse transition temperature T_θ which implies that if simulations are performed at this temperature the native conformation will not be stable at all. Fig. (9b) shows that T_f (the folding transition temperature) is once again one half that of T_f^{CSE}, indicating the importance of non-compact structures in this case.

In Fig. (10) we show the behavior of $< \chi > (T)$ and $\Delta\chi(T)$ for $B_0 = -2.0$ for another sequence. In this case the agreement between the exact results and that calculated using CS alone is significantly better. The difference between the two is roughly on the order of ten percent. These calculations clearly show that even in these models the importance of non-compact structures is dependent upon the value of B_0. Only for large values of $\mid B_0 \mid$ the low energy spectrum is dominated by CS alone.

3. Folding Kinetics: Kinetics of Approach to the Native Conformation

We begin with a discussion of the approach to the native state starting from an ensemble of disordered conformations. The kinetics of reaching the native state was monitored by studying the time dependence of $< \chi(t) >$ averaged over several initial conditions. For all the sequences that we have examined we find that $< \chi(t) >$ can be fit by a sum of exponentials after a transient time. In our previous studies using off-lattice models we had

shown that in general for a foldable sequence a fraction of initial population of molecules reaches the native state directly without encountering any discernible intermediates [44,50]. This is the case in these models as well, thus further supporting the conclusions of our earlier work which was based on Langevin simulations of off-lattice models. Since the data base analyzed here is more extensive, covering a wide span of σ, we can further classify the meaning of the various exponential terms that arise in the time dependence of the overlap parameter. In order to classify the various sequences in terms of the rapidity of folding to the native conformation we have used the parameter σ as a discrimination factor.

(a) Fast folding sequences ($\sigma \lesssim 0.1$):

For these sequences the structural overlap function $< \chi(t) >$ for t greater than a transient time is adequately fit by a single exponential, i.e.,

$$< \chi(t) > \simeq a_f \exp(-t/t_{TINC}). \tag{19}$$

In these cases the folding appears to be a two state all-or-none process and $\tau_f \approx \tau_{TINC}$, where τ_{TINC} is the time scale of topology inducing nucleation collapse (TINC). The folding and the collapse is almost synchronous. It has been shown in other studies that the folding for these sequences proceeds by a TINC mechanism [44,50–53]. In these studies the TINC mechanism was established by studying the microscopic dynamics of the trajectories. We found that once a critical number of contacts is formed (corresponding to a nucleus) the native conformation is reached rapidly. This fast folding is clearly observed when σ is less that 0.1.

(b) Moderate folding sequences ($0.1 \lesssim \sigma \lesssim 0.6$):

These are sequences when a single exponential fit cannot describe time course of the overlap function $< \chi(t) >$. We find that after an initial time, $< \chi(t) >$ is well fit by two exponentials. The interpretation of the fast and slow processes have been given elsewhere in our studies of continuum models using Langevin simulations [44,50]. The range of σ that characterizes moderate folding is $0.1 \lesssim \sigma \lesssim 0.6$. The onset of the intermediate values of σ is easy to obtain. This can be inferred by the smallest value of σ for which biexponential fit of $< \chi(t) >$ is

required to describe the approach to the native conformation.

(c) Slow folding sequences ($\sigma \gtrsim 0.6$):

These are sequences with $\sigma \gtrsim 0.6$. When σ gets close to unity, these sequences do not fold on any reasonable simulation time. If σ is greater than almost 0.6 we once again find that multiexponential fit to $< \chi(t) >$ is needed. The boundary between moderate and slow folding sequences is rather arbitrary. In both these cases we find that the various stages of folding can be described by a three stage multipathway mechanism (TSMM): The initial stage is characterized by random collapse, the second stage corresponds to the kinetic ordering regime in which the search among compact structures leads to native-like intermediates [33,44]. The final stage corresponds to activated transition from one of the native-like structures to the native state, which is the rate determining step for folding. Thus, the transition states occur close to the native conformation as was shown some time ago in off-lattice simulations [16,43]. Our earlier lattice and off-lattice studies describe in detail the evidence for the TSMM. Analysis of the trajectories probing the approach to the native state (measured by $\chi(t)$) for the sequences studied exhibits similar behavior.

4. Dependence of Folding Times on σ

In an earlier two dimensional lattice simulations we have suggested that the sequences that fold fast appear to have small values of $\sigma = (T_\theta - T_f)/T_\theta$ [33]. The reason for expecting the relationship between σ and the folding time τ_f has been given recently [34]. Physically if σ is small then $T_\theta \approx T_f$ and all possible transient structures that are explored by the chain on its way towards the native state are of relatively high free energy. Consequently, all the structures that are likely to act as traps or intermediates are effectively destabilized and thus folding to the native structure is rapid. For large σ T_f and T_θ are well separated and hence the chain searches many compact globular states in a rough energy landscape that leads to slow folding. When σ is small the folding process and the collapse is synchronous and this leads to fast folding. Similar conclusions have been reached for 2D square lattice

proteins [33,54].

In order to test the possible relationship between the folding time and σ we have calculated τ_f for the database of sequences generated by the method described in Sec. (II). The results of this simulations are plotted in Fig. (11) for $N = 15$ and $B_0 = -0.1$ (solid circles), $B_0 = -2.0$ (open circles). The figure shows that the folding time τ_f correlates statistically extremely well with the intrinsically thermodynamic parameter σ. The sequences span a range of σ and consequently meaningful conclusions can be made. In fact, sequences with small values of σ fold extremely rapidly (fast folding sequences): for σ smaller than 0.1, τ_f hardly exceeds 10^4 MCS. Most sequences (i.e., having σ between 0.15 and 0.6) have intermediate folding rates extending from roughly 10^5 to 10^7 MCS (moderate folding sequences). The sequences with the largest values of σ (greater than 0.6) are slow folding sequences, whose typical folding times are above 10^7 MCS. Thus, in the range of σ examined the folding rate changes by about four to five orders of magnitude. It is important to point out that all fast folding sequences are optimized, whereas moderate folding sequences also include random ones. Slow folding sequences are exclusively random. This distinction based on folding times and its dependence on σ was used in classification of the sequences in the discussion in Sec. (III.A.3).

5. Relationship between τ_f and Δ

Sali *et al.* have recently asserted (without providing explicit calculation of folding times) that sequences that fold rapidly and whose native conformation is also stable are characterized by large gap [20,21]. The gap in their model is defined using Eq. (18). In order to check this claim we plot τ_f as a function of Δ in Fig. (12) for $N = 15$. The corresponding plot for $N = 27$ is shown in the next section. Fig. (12) shows that this parameter is of little relevance when used to classify folding rates of different sequences. It appears that the sequences with large gaps Δ usually fold rather rapidly (about $10^4 - 10^5$ MCS). However, sequences having a small energy gap Δ can have either very small folding times (below 10^4

MCS) or do not reach native state even after $10^8 - 10^9$ MCS. For example, from Fig. (12) it is clear that if τ_f is fixed at 10^5 MCS then we can, in principle, generate a large number of sequences with very small values of Δ to very large Δ all with roughly the same τ_f. Thus, Δ alone cannot be used to discriminate between fast and slow folding sequences. The existence of large values of Δ/k_BT being a criterion for stability follows from Boltzmann's law with proteins being no exception.

6. Kinetic Events in the Folding Process

We have systematically investigated the microscopic processes that are involved in the folding of several sequences. This has been done by using the methodology for monitoring the intermediates described in Eqs. (16) and (17). We discuss the results of this study for the various sequences using the classification in terms of the parameter σ.

(a) Fast folders ($\sigma \lesssim 0.1$): In this case there are no well defined intermediates in the sense that the chain gets trapped in a conformation that is distinct from the native state for any length of time. For these fast folding sequences we find that the native conformation is reached by essentially a TINC mechanism, i.e. once a certain number of critical native contacts is established then the native state is reached rapidly [44,50,51]. By using a combination of Eqs. (16) and (17) we find that for fast folders the chain frequently visits the nearest low lying energy conformations even after reaching the native structure. For these sequences these low lying states are almost native-like (have about 90 percent of native contacts). In terms of the underlying energy landscape it is clear that they belong to the same basin of attraction as the native conformation.

(b) Moderate and slow folders ($\sigma \gtrsim 0.1$): These sequences appear to have well defined intermediates and their significant role makes folding in this range of σ quite distinct from the fast folders. In Fig. (13) we plot P_r and P_{fl} (see Eqs. (16,17)) for a variety of sequences. The sequences are arranged in order of increasing folding time. Recall P_r corresponds to the average probability that the intermediate with the energy E_k has the highest proba-

bility of occurrence before the native conformation is reached for the first time and P_{fl} is the average probability that this state is revisited after the native state is reached. This graph shows several striking features: (i) For moderate folders there is a finite probability of the chain revisiting the same intermediate that it sampled in the approach to the native conformation. This seldom happens in the sequences that fold slowly. It is clear that slow folding sequences have well defined intermediates which are not visited after the chain reaches the native conformation. These results suggest that the rate determining step in slow folding sequences is the transition from one of these intermediates to the native state. This involves overcoming a substantial free energy barrier. The existence of this barrier also prevents frequent excursions from the native state. (ii) It is of interest to probe the nature of intermediates that are encountered in the folding process. In Figs. (14a) and (14b) we show, respectively, the fraction of native contacts in the most populated intermediates and the corresponding overlap χ_k with native conformation for all sequences. For both fast and moderate folders it is clear that the states that are sampled have great structural similarity to the native conformation. In fact, in this case these conformations have roughly 80 percent of the native contacts. However, slow folding sequences have only about 50 percent of native contacts in the intermediate structures. It also turns out that in the case of moderate folders the most populated intermediates prior to formation of native conformation is most often the first excited state whereas in slow folding sequences it is the higher excited states that have the largest probability of occurring. (iii) The rate of formation of the intermediates can be ascertained by examining Fig. (14c), in which the ratio of the mean time to reach the intermediate τ_k to the folding time τ_{fp} is plotted. Intermediates for fast and moderate folding sequences usually occur at later stages of folding than for slow folding sequences. In fact, for the latter cases the ration τ_k/τ_{fp} can be as low as 0.1. This implies that these relatively stable misfolded structures are formed relatively early in the folding process and these off-pathway processes therefore slow down the folding considerably. It also follows that the rate determining step for slow folders occurs late in the folding process implying that the transition states are closer to the native structure [43].

B. $N = 27$: $B_0 = -0.1$ and $B_0 = -2.0$

For $N = 27$ we have generated 15 sequences with $B_0 = -0.1$ using the optimized design procedure described in Sec. (II.E). In this case all of the sequences have been optimized so that σ is in the range of $\sigma \lesssim 0.12$. We have studied the thermodynamic properties of few sequences with $B_0 = -2.0$. Since we have already established that non-compact structures make significant contribution to both the thermodynamic and kinetic properties for $N = 15$ it is necessary to include them in studying the case of $N = 27$ as well. The number of non-compact structures for $N = 27$ is of the order of 10^{18} and their exact enumeration is impossible. We have, therefore, used slow cooling Monte Carlo method (see Appendix A) to calculate the thermodynamic properties in this case. The calculation of the kinetic processes have been done as before for $N = 15$. We discuss there results below. Since the qualitative behavior remains the same we provide a less detailed account for this case.

1. Thermodynamic Characteristics

As before we have determined T_θ and T_f from computing the temperature dependence of C_v and $\Delta\chi$. The simulation temperature was found by requiring that the overlap function $< \chi(T_s) >= 0.21$. These temperatures were calculated using Monte Carlo simulations. It is interesting to compare the results for the overlap function obtained from MC simulations with that calculated using CSE only (Figs. (15,16)). The results for the temperature dependence of $\Delta\chi$ for one sequence with $B_0 = -0.1$ is given in Fig. (15b) and in Fig. (16b) $\Delta\chi$ as a function of T is plotted for another sequence with $B_0 = -2.0$. The dotted line in these figures are the results obtained using the contribution of compact structures only. Both these sequences have large values of the energy gaps Δ. These figures show dramatically that the neglect of noncompact structures leads to serious errors in the determination of $\Delta\chi$. Similar discrepancies are found for other thermodynamic quantities as well. The errors in the estimate of T_f in these two sequences are about a factor of 2 - 3. In fact, in both cases the

estimate of T_f^{CSE} obtained using compact structures alone exceeds the collapse transition temperature T_θ. The neglect of noncompact structures, even for $B_0 = -2.0$, results in more serious errors than for $N = 15$. In any event for both $N = 15$ and $N = 27$ restriction to compact structures alone can lead to incorrect results for thermodynamic properties.

It is interesting that the discrepancy between the simulation temperature T_s^{MC} and T_s^{CSE} is even more dramatic for $N = 27$ at the value of $B_0 = -0.1$ (Fig. 15a). In particular, for the sequence 61 for which $\Delta\chi(T)$ is displayed in Fig. (15b) $T_s^{CSE} = 3.19$, which is even larger than $T_\theta^{MC} = 1.22$, exceeds $T_s^{MC} = 1.17$ by almost a factor of three. As expected for $B_0 = -2.0$ the discrepancy is somewhat smaller but is still very significant (see Fig. (16a)). In this case $T_s^{CSE} = 3.60$ is almost twice as large as $T_s^{MC} = 2.06$. The value of T_θ for this sequence is $T_\theta^{MC} = 2.14$. This implies that, if the simulation temperatures T_s^{CSE} are used, the only conformations that are thermodynamically relevant are the random coil ones. These observations clearly demonstrate that the use of only compact structures for calculating thermodynamic quantities is in general totally flawed and would lead to incorrect evaluation of the folding rates for both $B_0 = -0.1$ and $B_0 = -2.0$ for any N. It is worth noting that a similar conclusion has been reached for a two letter code model with $N = 27$ [55].

In Fig. (17) we collect the results for the ratio of the simulation temperature calculated using compact structures T_s^{CSE} to that computed using all available conformations T_s. For the case of $N = 27$ we have already emphasized that the simulation temperature (denoted as T_s^{MC}) is calculated using Monte Carlo simulations the details of which are examined in Appendix A. In Fig. (17a) we show the ratio T_s^{CSE}/T_s^{FE} for $N = 15, B_0 = -0.1$. It is clear that except for one sequence this ratio is greater than unity and is large as 2.5. The results T_s^{CSE}/T_s^{MC} for $N = 27, B_0 = -0.1$ are displayed in Fig. (17b). Here the effects are even more dramatic. In all cases this ratio exceed 2.0 implying that noncompact structures make significant contributions in determining thermodynamic properties.

A further consequence of using only compact structures to determine T_s (as has been done elsewhere [20,21]) is that at these high temperatures the native conformation has no

stability. It is because of the very large values of T_s^{CSE}, Sali *et al.* find that in many cases their native conformations are not well populated. In fact, in most cases the probability of being in the native conformation is less than 0.1.

2. Folding Kinetics: $N = 27$ *and* $B_0 = -0.1$

Since the time scales for folding for $N = 27$ are quite long we have restricted ourselves to determining the folding rates for optimized sequences only. Thus, we have examined 15 sequences with characteristic temperatures T_θ and T_f that provide the values of σ being less than about 0.12. These sequences, according to the classification derived at detailed study of $N = 15$, would all be the fast folders. Thus, we expect that most of these sequences would reach the native conformation extremely rapidly. In these instances folding would appear to be a two state all-or-none process and the time dependence of $< \chi(t) >$ should be exponential. All these expectations are borne out. In Fig. (18a) we show $< \chi(t) >$ for one of the sequences from fifteen examined. It is obvious that $< \chi(t) >$ is well fit by a single exponential process.

For some sequences we do find that $< \chi(t) >$ can be better fitted by a sum of two exponentials. Thus, for $N = 27$ even for these small values of σ we find that these sequences should be classified as moderate folders (Fig. (18b)). This is not surprising because as N increases the probability of forming misfolded structure also increases. The boundaries differentiating the fast and moderate folders depend on the sequence length. For large values of N the range of σ over which the sequences behave as fast folders decreases. Consequently, the partition factor $\Phi(T)$, which is the fraction of initial population of molecules that reaches the native conformation *via* TINC mechanism, decreases.

3. Dependence of Folding Times on σ, Δ, *and* Δ_{CS}

The dependence of the τ_f on σ is shown in Fig. (19). Even though we have examined only a small range of σ the general trend that τ_f is well correlated with σ is clear. Considering

that one has statistical errors in determining both σ and τ_f the observed correlation between these quantities is, in fact, remarkable. In this limited range of σ the folding time changes by nearly a factor of 300 indicating that small changes in σ (which is an intrinsic property of the sequence) can lead to rather large changes in τ_f. The behavior of τ_f on Δ is shown in Fig. (20). The trend one notices is the same as in the case of $N = 15$. In fact, the lack of any correlation between τ_f and Δ is even more apparent here. As in the case for $N = 15$ it is possible to generate sequences with arbitrary values of the gap that would all have roughly the same folding time. Notice that although σ covers only a small range the gap extends over a much wider interval. This also implicitly indicates no dependence of σ on Δ.

If there would be any plausible relation between τ_f and Δ it is clear that Δ has to be expressed in terms of a suitable dimensionless parameter. Unfortunately the proponents of the energy gap idea [20,21] as the discriminator of folding sequences have used varying definitions of Δ in different papers without providing the precise way this is to be made dimensionless. The energy parameter that would make Δ dimensionless cannot be B, the standard deviation in the distribution of contact energies which merely sets the energy scale, because this would mean this criterion would apply only to this model. The gap Δ in Figs. (12) and (20) is measured in units of B. A very natural way to make Δ dimensionless is to divide it by k_BT which is in this case k_BT_s. In Fig. (21) we have presented the folding times τ_f as a function of Δ/T_s. The upper panel is for $N = 15$, while the lower one is for $N = 27$. These figures demonstrate even more dramatically the irrelevance of Δ/T_s as a parameter in determining folding times. In fact, this figure is almost like a scatter plot. Thus, it is clear that energy gap alone (measured in any suitable units) does not determine folding times in these models. From this it follows that the classification of sequences into fast and slow folders cannot be done using the value of Δ (measured in any reasonable units) alone.

In the literature it has been forcefully asserted that foldability of sequences in this class of models is determined by Δ_{CS}, the energy gap for the ensemble of compact structures [20,21]. Plotting τ_f as a function of Δ_{CS} for our model appears to be somewhat ambiguous because about half of the sequences have non-compact native conformations. In Fig. (22)

we plot τ_f as a function of Δ_{CS}. The upper panel is for $N = 15$ and the lower panel is for $N = 27$. It is clear from this figure that there is no useful correlation between τ_f and Δ_{CS}. It appears that one can generate sequences with a range of Δ_{CS} all of which have roughly the same folding times.

C. Kinetic Accessibility and Stability of Native Conformation

It is well known that many natural proteins reach their native conformation quite rapidly without forming any detectable intermediates. However, proteins are only marginally stable in the sense the equilibration constant K for the reaction

$$U \rightleftharpoons F \tag{20}$$

is only between $10^4 - 10^7$. In Eq. (20) U refers to the denaturated unfolded conformations, and F is the folded native state. Thus, $\Delta G = G_F - G_U = -k_B T ln K$ is in the range of $-12k_BT$ to $-18k_BT$. While this is not as large as one observes in typical chemical reactions involving cleavage of bonds it is still sufficiently large so that the native conformation is overwhelmingly populated relative to the ensemble of unfolded states. The Helmholtz free energy of stabilization of the folded state with respect to the ensemble of denaturated conformations can be written as

$$\beta \Delta F \simeq -\Delta E + S_U \tag{21}$$

where ΔE is the stabilization energy, S_U is the entropy of the ensemble of the unfolded structures. We have assumed that the conformational entropy associated with the native conformation is negligible. If the ensemble of denaturated structures corresponds to self-avoiding random walks S_U for lattice models can be estimated using Eq. (4). For cubic lattice $Z_{eff} = 4.684$, $\gamma = 1.16$, and thus $\beta \Delta F \simeq -\Delta E + 42$ for $N = 27$. If we insist that $\beta \Delta F \approx 10$ this would imply that $\Delta E(T) \approx -52 k_B T$. The same calculations would show that $\Delta E(T) \approx -20 k_B T$ if the ensemble of structures in the denaturated states are

essentially compact structures. This estimate is a bit more realistic. These estimates show that the native conformation is overwhelmingly populated under appropriate conditions relative to the compact structures. More recent experimental studies involving denaturant induced unfolding of few proteins have been used to probe the "spectrum" of low free energy conformations [56]. These tools, while being relatively primitive, suggest that typically the equilibrium intermediates are also about $6 - 8k_BT$ higher in free energy than the native conformation. Thus, even in these cases, under native conditions, the native state is overwhelmingly (≥ 0.9) occupied.

Most of the simulations we have discussed so far have been done at temperatures below T_f but high enough that the $< \chi(T_s) >$ is as large as possible. This, of course, has been done for computational reasons and the constant value of $< \chi(T_s) >$ has been chosen so that the properties of different sequences can be compared on equal footing. However, at these simulation temperatures T_s the probability of occupation of the native conformation $P_{nat}(T_s)$ varies between 0.2 and 0.6, which is significantly smaller than what is observed in real proteins. Notice that the calculations of Sali *et al.* [20,21] have been done at such elevated temperatures that the probability of occupation of native conformation for two hundred sequences examined is usually between $0.01 - 0.05$ and none exceeds 0.4. Thus, these authors, although have stated the criterion for simultaneously satisfying kinetic accessibility and stability (this follows from Boltzmann's law), did not provide <u>any</u> computational or theoretical evidence that <u>any</u> of their sequences obeyed the stated criterion at any temperature.

In light of the above arguments it is necessary to use a different criterion for the choice of T_s which would ensure stability of the native proteins. Accordingly, we have performed simulations for a few sequences with $N = 15$ and $B_0 = -0.1$ at the temperatures which are determined using the following equation

$$\eta(T_{s\eta}) = 1 - P_{nat}(T_{s\eta}) = c \tag{22}$$

where $P_{nat}(T_{s\eta})$ is the probability of the chain being in the native conformation at $T = T_{s\eta}$. The constant c was chosen to be equal to 0.1, which implies that probabil-

ity of the chain being in the native conformation is 0.9. In order to present the contrast between the kinetic behavior of the sequences at temperatures chosen using Eq. (22) $T_{s\eta}$ we chose three sequences one from fast folders ($\sigma \lesssim 0.1$), one from moderate folders ($0.1 \lesssim \sigma \lesssim 0.6$), and one from slow folders ($\sigma \gtrsim 0.6$). The ratios of the simulation temperatures for these sequences $T_{s\eta}$ determined using Eq. (22) to T_s obtained using the overlap criterion are approximately 0.5, 0.6, and 0.6 for fast, moderate, and slow folders, respectively. It appears that stability of the native conformation (occupancy of this state ≥ 0.8) for both fast and moderate folders can be achieved, if the simulation temperature T_s is taken to be one half of the folding temperature T_f.

The quantity $\eta(T)$ should only be the function of $T/T_{s\eta}$ if the gap between the native conformation and the first excited state is large. More precisely, we expect this to be valid for all temperatures such that $k_BT \ll \Delta$, where Δ is the gap, separating the energy of the native conformation and the first excited state. To see this $\eta(T)$ can be written as

$$\eta(T) \simeq \frac{\exp(-\frac{\Delta}{k_BT})}{1+\exp(-\frac{\Delta}{k_BT})} \tag{23}$$

for $\Delta/k_BT \gtrsim 1$. The temperature $T_{s\eta}$ is determined from Eq. (22) and thus $\eta(T)$ becomes

$$\eta(T) = f(T/T_{s\eta}) \simeq \frac{y^{1/\tau}}{1+y^{1/\tau}}, \tag{24}$$

where $y = c/(1-c)$ and $\tau = T/T_{s\eta}$. This is confirmed in Fig. (23), where plots of η as a function of $T/T_{s\eta}$ are shown for three sequences. Two of them follow the behavior in Eq. (24) for $T/T_{s\eta} < 1.5$, whereas the sequence with small gap ($\Delta/k_BT_{s\eta} < 1$) does not.

The behavior of $< \chi(t) >$ and the fraction of unfolded molecules $P_u(t)$ as a function of time for two of the sequences is shown in Figs. (24) and (25). The temperature for the third sequence was so low for Eq. (22) to be satisfied that the folding time for this sequence was estimated to be in excess of 10^{10} MCS. By studying these graphs we draw the following conclusions: (i) The overlap function $\chi(t)$ at the low temperature (Fig. (24a)) is clearly biexponential, whereas at $T = T_s$ (see Eq. (11)) the folding process was an all-or-none process. This is because the very small barrier ($\delta E^{\ddagger} \simeq k_BT_s$) becomes discernible

at $T \simeq T_{s\eta}$. This fact alone would yield to the prediction that τ_f at $T_{s\eta}$ should be about a factor of 10 larger. This is consistent with simulation results. So the emergence of the second component in $P_u(t)$ (Fig. (24b)) is due to the activated transition from the first excited state to the native conformation. The behavior of $\chi(t)$ for the moderate folding sequence is qualitatively similar to that at $T = T_s$ except that the time constants are larger because $T_{s\eta} \approx \frac{1}{2}T_s$ (Fig. (25)). (ii) We find that the ratio of the folding times for the three sequences at $T = T_{s\eta}$ is roughly the same as found at $T = T_s$. This suggest that although the overall folding times have increased considerably we do not expect to see qualitative differences in the fundamental conclusion regarding the statistical correlation between τ_f and σ. (iii) Examination of the fraction of unfolded molecules $P_u(t)$ shows that the biexponential behavior is consistent with the kinetic partitioning mechanism [44]. A fraction of the molecules, $\Phi(T)$, reaches the native state very rapidly without forming any intermediates *via* TINC mechanism, while the remainder follows a more complex kinetic mechanism. The partition factor $\Phi(T)$ is nearly unity for fast folding sequences at $T = T_f$ leading to a two state behavior, whereas at low temperatures $\Phi(T) < 1$. For fast folding sequences shown in Fig. (24b) $\Phi(T = T_{s\eta})$ is approximately 0.4. In the case of moderate folders $\Phi(T)$ is always less than one for all $T < T_f$. This is affirmed in Fig. (25b), where we find that $\Phi(T = T_{s\eta})$ is approximately 0.19 for the sequence with $\sigma = 0.19$.

IV. CONCLUSIONS AND DISCUSSION

In recent years there have been numerous studies of lattice models of proteins, in which the protein is modeled as a self-avoiding walk on a three dimensional cubic lattice. A variety of interactions between the beads on this lattice has been studied. In this work we have carried out a systematic investigation of the kinetics and thermodynamics of a heteropolymer chain confined to a cubic lattice under a variety of conditions. We have, as majority of the studies have in the past, used a random bond model to specify the interaction between the beads. Specifically the interactions between the beads are chosen

from a Gaussian distribution of energies with a non-zero value of the mean B_0. In order to obtain a coherent picture of folding in this highly simplified representation of proteins we have studied the kinetic and thermodynamic behavior for two values of N (the number of beads in the chain), namely $N = 15$ and $N = 27$. For $N = 15$ the thermodynamic characteristics can be exactly calculated because all possible conformations in this case can be exhaustively enumerated, whereas for $N = 27$ all the quantities of interest have to be obtained by Monte Carlo simulations. In addition the mean hydrophobic interaction B_0 has also been varied in this work. The kinetics of folding for a number of sequences have been obtained by Monte Carlo simulations. The work reported here allows us to assess the various factors that govern folding in this model. In addition the variation in parameters can be used to address some of the proposals made earlier in the literature.

The exact calculations for $N = 15$ of the thermodynamic quantities by enumerating all the conformations clearly demonstrate the importance of non-compact structures in determining accurately the characteristic properties of the protein chain. For $B_0 = -0.1$, which is a realistic value for proteins (see Sec. (II.B)), the values of the temperatures T_θ (the collapse transition temperature) and T_f (the folding transition temperature) are much higher, if only the compact structure are included. This, in turn, makes the simulation temperature T_s (see Eq. (11)) also quite high. In fact for most sequences T_s determined using only the compact conformations exceeds T_θ. Although the discrepancies between T_s determined using CS and all the conformations for $B_0 = -2.0$ (a rather unrealistic value for proteins) is lesser the resulting kinetics is significantly affected. However, for $N = 27$ the differences between T_s found from CSE and that determined from Monte Carlo simulations are very significant even for $B_0 = -2.0$. The two values in some instances differ by a factor of two. Thus if the simulation temperature is chosen using only compact structures that is much more convenient, then one obtains a value for T_s that often exceeds the collapse transition temperature. This fact alone explains why the probability of occupancy of the native state was very small (in many cases less than 0.1) in the previously reported studies in the literature [20,21]. It has been pointed out by Chan [29] that the high temperatures used by Sali *et al.* [20,21]

results in the equilibrium population of the native conformation for 'folding sequences' of only $0.01 - 0.05$ with none exceeding 0.4. This was not appreciated by Sali *et al.* because they used a very crude criterion for folding. In particular a sequence was designated as a folding sequence if at the temperature of simulation the native conformation was reached once (a first passage time) at least four times among ten independent trajectories of maximum duration of 50×10^6 MCS [21]. Our studies indicate that ten trajectories is absolutely inadequate for obtaining even qualitatively reliable estimate of any property of interest.

We had shown earlier in lattice and off-lattice studies [28,33,44] that the two temperatures that are intrinsic to a given sequence are T_θ and T_f. This general thermodynamic behavior for protein-like heteropolymers has been confirmed recently [55]. In addition the temperature of simulation (or experiment) should be below T_f so that the folded state is the most stable. Theoretical arguments suggest [34] that the parameter $\sigma = (T_\theta - T_f)/T_\theta$ is a useful indicator of kinetic foldability in the models of the sort considered here, and perhaps in real proteins as well. By examining the kinetics of approach to the native conformation we have found that roughly (this holds good for $N = 15$) the kinetic foldability of sequences can be divided into three classes depending on the value of σ. For $N = 15$ we find that fast folders have σ less than about 0.1, moderate folders have σ in the range of approximately 0.1 and 0.6, while σ values greater than about 0.6 correspond to slow folders. It should be emphasized that the ranges for these three classes of sequences depend on the length of the chain: longer chains have smaller range of σ for fast folding. Fast folding sequences can kinetically access their ground state at relatively higher temperature compared to slow folding sequences. The kinetics of approach to the native state differs significantly between fast folding sequences and those that are moderate folding sequences. In the former case the native conformation is reached via a TINC mechanism and there are no detectable intermediates. In this case the folding appears as an all-or-none process. The kinetics is essentially exponential. On the other hand the moderate folding sequences reach the native conformation (predominantly) via a three stage multipathway mechanism as was reported in our several earlier studies.

The time dependence of the approach to the native conformation is very revealing. For

moderate folding sequences the simulation temperature is lower than for sequences with small σ. Thus if approach to the native conformation with the same value of the overlap function is examined we find that the moderate folding sequences follow the kinetic partitioning mechanism (KPM) [44,50]. This implies that a fraction of the initial population of molecules reaches the native state via the TINC mechanism while the remaining one follows the three stage multipathway process. The partition factor, $\Phi(T)$, that determines the fraction that follows the fast process is sequence and temperature dependent. Thus even fast folding sequences, which would have $\Phi(T)$ close to unity at higher temperature, would have fractional values less than unity at lower temperature. This is clearly seen in Fig. (24b). This work suggests that KPM should be a generic feature of foldable proteins. The partition factor can be altered by mutations, temperature, and by changing other external factors such as pH.

We have explicitly calculated the folding times for a number of sequences for the various parameters (different N and B_0) values. This is of great interest to examine whether there is any intrinsic property of the sequences that can be used to predict if a particular sequence folds rapidly or not. It has been argued based on the random energy model for proteins that folding sequences should have as large a value of T_f/T_g as possible, where T_g is an equilibrium glass transition temperature [1,31]. Kinetic studies of lattice models of proteins suggest that this criterion may be satisfied for foldable sequences provided T_g is substituted by a kinetic glass transition temperature which is defined as the temperature at which folding time scale exceeds a certain arbitrary value [21]. Scaling arguments have been used to suggest that there should exist a correlation between folding times and σ [33,34]. More recently it has been emphatically stated in the form of a theorem (without the benefit of explicit computations) that the necessary and sufficient condition for rapid folding in the models studied here is that there should be a large gap (presumably measured in units of k_BT) between the lowest energy levels. The calculations of folding times reported here clearly show that there is no useful correlation between the gaps and folding times for any parameter values that we have investigated. In fact for a specified folding time one can engineer sequences with both large

and small values of the gap. Thus the precise value of the gap alone cannot discriminate between folding sequences. On the other hand there is a good correlation between the folding times for sequences and σ. It is clear that sequences with small values of σ have short folding times, while those with larger values have higher folding times. It should be emphasized here that the criterion based on σ should only be used to predict trends in the folding times. In this sense this criterion should be used in a qualitative manner. The major advantage of showing the correlation between σ and the folding times is that σ can be experimentally determined. The folding transition temperature is nominally associated with the midpoint of the denaturation curve while T_θ is the temperature at which the protein resembles a random coil.

In the usual discussion of protein folding only the issue of kinetic foldability of sequences are raised. Since natural proteins are relatively stable (this does not imply that the protein does not undergo fluctuations in the native conformation) with respect to both the equilibrium intermediates and the ensemble of unfolded conformations it is imperative to devise the criterion for simultaneously satisfying kinetic accessibility of the native conformation and the associated stability. This paper for the first time has provided an answer to this issue. It is clear from our study that fast folders have small values of σ, and consequently designing proteins [33,57] using this criterion assures kinetic accessibility of the native conformation at relatively high temperature. For example, if T_θ is taken to be about $60^\circ C$ then the fast folders would reach the native conformation rapidly even at temperatures as $55^\circ C$ ($\sigma \approx 0.1$). However, at these temperatures the native conformation may not be very stable, i.e. the probability of being in the native conformation may be less than 0.5. On the other hand, if these fast folders are maintained at $T \approx (0.5 - 0.6)T_f \approx (30 - 35)^\circ C$ for $\sigma \approx 0.1$ and $T_\theta \approx 60^\circ C$ then both kinetic accessibility as well as stability can be simultaneously satisfied.

Our simulations also suggest that the dual criterion can also be satisfied by using moderate folders. In these cases we find that the native state is reached relatively rapidly at low enough temperatures ($T \approx (25 - 30)^\circ C$ assuming $T_\theta \approx 60^\circ C$) at which the excursions to other conformations are not very likely. In the extreme case of very slow folders we find

(see Fig. (26)) that the average fluctuation probability of leaving the native conformation after initially reaching it is small, i.e. the stability condition is easily satisfied. In these cases however the kinetic accessibility is, in general, not satisfied. From these observations it follows that in order to satisfy the dual criterion it is desirable to engineer fast folders (small values of σ) and perform folding at temperatures around $(0.5-0.6)T_f$. Alternatively, one can use moderate folders at temperatures around $0.8T_f$. Since moderate folders are more easily generated (by a random process) it is tempting to suggest that many natural proteins specifically large single domain proteins may be moderate folders.

Finally, we address the applicability of the results obtained here to real proteins. Since many features that are known to be important in real proteins (such as side chains, the possibility of forming secondary structures etc.) are not contained in these models the direct applicability to real proteins is not clear. Nevertheless simulations based on other more realistic minimal models together with theoretical arguments can be used to suggest that the scenarios that have emerged from this and other related studies should be observed experimentally. In particular it appears that the kinetic partitioning mechanism which for most generic sequences is a convolution of the topology inducing nucleation collapse mechanism and the three stage multipathway kinetics should be a very general feature of protein folding in vitro. The theoretical ideas developed based on these minimal models also suggest that the partition factor $\Phi(T)$ is a property of the intrinsic sequence as well as external factors such as temperature, pH etc. In fact recent experiments on chymotrypsin inhibitor 2 (CI2) suggest that this KPM has indeed been observed [53]. In this particular case Otzen *et al.* have observed that CI2 reaches the native state immediately following collapse. This, in the picture suggested here and elsewhere [44], would imply that in the case of CI2 under the conditions of their experiment ($T = 25^{\circ}C$ and pH = 6.2) the native conformation is accessed via a TINC mechanism. Moreover, the partition factor $\Phi(T = 25^{\circ}C)$ is close to unity making CI2 under these conditions a fast folder. If we assume that $T = 25^{\circ}C \approx T_f/2$ then it follows that for CI2 the value of σ is roughly 0.15. On the other hand these authors have also noted that for barnase the rate limiting step comes closer to the native state

involving the rearrangement of the hydrophobic core. They suggest in the form of a figure (see Fig. (3) of Ref. 52) that barnase follows a three stage kinetics with the rate determining step being the final stage. In terms of the physical picture suggested here this can be interpreted to mean that for barnase $\Phi(T)$ is small making it either a moderate folder or even a slow folder. If this were the case our theoretical picture would suggest σ for barnase is bigger which is a consequence of the fact that it is a larger protein. These observations are consistent with the experimental conclusions of Otzen *et al.* which are perhaps the first experiments that seem to provide some confirmation of the theoretical ideas that have emerged from the minimal model studies. It is clear that a more detailed comparison of the entire kinetics for various proteins under differing experimental conditions is required to fully validate the general conclusions based on the kinetic partitioning mechanism together with the classification of sequences based on the values of the parameter σ.

ACKNOWLEDGMENTS

This work was supported by a grant from the Airforce Office of Scientific Research (through grant number F496209410106) and the National Science Foundation. One of us (DT) is grateful to P.G. Wolynes and J.N. Onuchic for a number of interesting discussions.

APPENDIX A:

It is clear from our studies for $N = 15$, for which all conformations (compact and noncompact) can be exactly enumerated that the neglect of noncompact structures leads to qualitatively incorrect results for thermodynamic and kinetic properties at all temperatures. However for $N = 27$ the enumeration of all possible conformations is out of reach. Thus one has to resort to numerical methods to obtain as accurate results as possible. We have used a combination of slow cooling technique in conjunction with Metropolis Monte Carlo method to calculate several thermodynamic characteristics of the system. We have used similar algorithms in our studies on continuum models of β-barrel and four helix bundles

[44,58]. In this appendix we describe the algorithms that have been used to obtain the collapse transition temperature T_θ and the folding transition temperature T_f.

For a given sequence we first estimate the approximate temperature range which includes T_θ and T_f (and also T_s, at which $< \chi(T_s) >= 0.21$). To obtain this temperature interval, $T_l < T_s < T_f < T_\theta < T_h$, we quench the system starting from a random unfolded conformation (from an arbitrary self-avoiding conformation) to a high enough temperature T_h. In the first phase of the algorithm a few trajectories are generated so that approximate estimates of T_θ and T_f can be made. This allows us to pin the interval (T_l, T_h). This temperature interval spans the peaks of C_v and $\Delta\chi$ from which the characteristic temperatures are obtained. Starting from a given initial conformation at T_h the following linear cooling schedule was applied to lower the temperature

$$T_i = T_h - i\Delta T \tag{A1}$$

where i labels the i^{th} step in the slow cooling process and ΔT is the cooling rate. The initial conformation for the $(i+1)^{\text{th}}$ iteration is the final conformation at the end of the i^{th} step. At each step of the slow cooling process we run Monte Carlo simulations for the time τ_{max}. For the computation of equilibrium quantities we reject the conformations for a certain length of time τ_{eq} immediately after quench to a new temperature. This allows for the chain to equilibrate at that temperature. The precise value of τ_{eq} clearly is temperature dependent. In our simulations we chose a large enough value of τ_{eq} so even at the lowest temperatures it is sufficient for equilibration. Thus at each temperature the time averaged property of any quantity of interest, A, can be calculated as

$$A_j(T_i) = \frac{1}{\tau_{max} - \tau_{eq}} \int_{\tau_{eq}}^{\tau_{max}} A_j(s, T_i) ds, \tag{A2}$$

where j labels the initial trajectory generated at T_h. The true thermodynamic value $< A(T) >$ is obtained by averaging over an ensemble of initial conditions, i.e.

$$< A(T_i) >= \frac{1}{M} \sum_{j=1}^{M} A_j(T_i) \tag{A3}$$

In using Eqs. (A2) and (A3) we have assumed that the weights associated with the initial trajectories are uniform. This will only be valid provided there is not significant amount of multivalley structure in the potential energy surface. Since for $N = 27$ we have used only optimized sequences this assumption appears reasonable. Furthermore we have also checked that the same values of the thermodynamic properties are obtained in the limit of long times in the kinetic simulations as well. This again assures us that the computations based on the above procedure yield accurate values of all quantities of interest for the sequences examined.

In our simulations we chose $\tau_{eq} = 50,000$ MCS, $\tau_{max} = 10^6$ MCS, and the cooling rate $\Delta T = 0.01$. This value of ΔT was small enough so that the changes in the thermodynamic quantities in between two successive temperatures were less than the fluctuations at these temperatures. Specifically this choice ensures us that $< \chi(T_i) > - < \chi(T_i - \Delta T) > \ll (\Delta\chi(T_i))^{1/2}$. After the determination of $< \chi(T_i) >$, $< E(T_i) >$, $C_v(T_i)$, $\Delta\chi(T_i)$ for all $i(= 0, 1, 2...)$ using the above protocol they were fitted to appropriate polynomials or in the case of $< \chi(T) >$ to sum of two hyperbolic tangents. These functions were used to obtain T_θ and T_f for fifteen sequences with $B_0 = -0.1$ and for two sequences with $B_0 = -2.0$. The later calculations were done merely to check the role of non-compact structures in determining thermodynamic properties for $N = 27$ at a larger value of the overall hydrophobic interaction.

APPENDIX B:

In this appendix we describe the methods used to obtain the low energy spectrum of the sequences with $N = 27$. The sequences for this case were all optimized using the procedure described in Sec. (II.E). For a given primary sequence we first determined a set of low energy structures using the algorithm described in Appendix A. The lowest of these energy structure was then used as the target structure and an optimized sequence that is fitted to this target structure was generated. Typically the target structures contained between 22 to

28 (the maximum being 28) topological contacts. This procedure was repeated with another primary sequence until all the sequences are generated.

The lowest energy obtained in the design procedure was assumed to be the ground state of the designed sequence. We did not, during the course of our simulations, find any counter examples to this. Thus the native energy is determined in the process of sequence design itself. In order to obtain the other energy levels we used a slow cooling Monte Carlo simulation starting from a high temperature T_h. The details of this protocol are given in Appendix A. During the course of this slow cooling simulations the energy $E(t, T_i)$ is monitored for all values of t and T. These energies were then arranged in increasing order thus yielding the spectrum for one given sequence. In order to ensure that the energies are truly equilibrium spectrum this procedure was repeated for several distinct initial conditions (namely, for $M = 100$). The simulation time for each sequence ranged from 5×10^7 to 6×10^7 MCS.

The procedure described here works best for the determination of the gap Δ, when the temperature T_l is low enough so that one essentially has a two level system. Since the sequences are all optimized most of the values of Δ are reasonably large that this never is the problem. There were few sequences with relatively small values of Δ. In these cases we also performed slow warming simulations starting from T_l. Once again the energy as a function of time was recorded and we obtained exactly the same results for Δ. Thus it is extremely unlikely that there are any significant errors at least in the determination of Δ.

REFERENCES

[1] Bryngelson, J.D., Onuchic, J.N., Socci, N.D., Wolynes, P.G. Funnels, pathways and the energy landscape of protein folding: A synthesis. Proteins Struct. Funct. Genet. 21:167-195, 1995.

[2] Dill, K.A., Bromberg, S., Yue, K., Fiebig, K.M., Yee, D.P., Thomas, P.D., Chan, H.S. Principles of protein folding - A perspective from simple exact models. Protein Sci. 4:561-602, 1995.

[3] Hinds, D.A., Levitt, M.A. Exploring conformational space with a simple lattice model for protein structure. J. Mol. Biol. 243:668-682, 1994.

[4] Karplus, M., Shakhnovich, E. Protein folding: Theoretical studies of thermodynamics and dynamics. In: "Protein Folding". Creighton, T.E., (ed.). New York: W.H. Freeman. 1992:127-196.

[5] Thirumalai, D. Theoretical perspectives on in vitro and in vivo protein folding. In: "Statistical mechanics, protein structure, and protein substrate interactions". Doniach, S., (ed.). New York: Plenum Press. 1994:115-133.

[6] Wolynes, P.G., Onuchic, J.N., Thirumalai, D. Navigating the folding routes. Science 267:1619-1620, 1995.

[7] Baldwin, R.L. The nature of protein folding pathways: The classical versus the new view. J. Biomolecular NMR 5:103-109, 1995.

[8] Radford, S.E., Dobson, C.M. Insights into protein folding using physical techniques: Studies of lysozyme and alpha-lactalbumin. Phil. Trans. Roy. Soc. Lond. B 348:17-25, 1995.

[9] Levinthal, C. In: "Mossbauer spectroscopy in biological systems". Debrunner, P., Tsibris, J.C.M., Münck, E. (eds.). Urbana: University of Illinois Press. 1969:22-24.

[10] Amara, P., Straub, J.E. Folding model proteins using kinetic and thermodynamic annealing of the classical density distribution. J. Phys. Chem. 99:14840-14853, 1995.

[11] Bryngelson, J.D., Wolynes, P.G. Intermediates and barrier crossing in a random energy model (with application to protein folding). J. Phys. Chem. 93:6902-6915, 1989.

[12] Chan, H.S., Dill, K.A. Energy landscapes and the collapse dynamics of homopolymers. J. Chem. Phys. 99:2116-2127, 1993.

[13] Chan, H.S., Dill, K.A. Transition states and folding dynamics of proteins and heteropolymers. J. Chem. Phys. 100:9238-9257, 1994.

[14] Covell, D.G., Jernigan, R.L. Conformations of folded proteins in restricted spans. Biochemistry 29:3287-3294, 1990.

[15] Hinds, D.A., Levitt, M.A. A lattice model for protein structure prediction at low resolution. Proc. Natl. Acad. Sci. USA 89:2536-2540, 1992.

[16] Honeycutt, J.D., Thirumalai, D. Metastability of the folded states of globular proteins. Proc. Natl. Acad. Sci. USA 87:3526-3529, 1990.

[17] Guo, Z., Thirumalai, D., Honeycutt, J.D. Folding kinetics of proteins: A model study. J. Chem. Phys. 97:525-535, 1992.

[18] Garel, T.R., Orland, H. Mean field model for protein folding. Europhys. Lett. 6:307-310, 1988.

[19] Leopold, P.E., Montal, M., Onuchic, J.N. Protein folding funnels: A kinetic approach to the sequence-structure relationship. Proc. Natl. Acad. Sci. USA 89:8721-8725, 1992.

[20] Sali, A., Shakhnovich, E., Karplus, M. How does a protein fold. Nature 369:248-251, 1994.

[21] Sali, A., Shakhnovich, E., Karplus, M. Kinetics of protein folding: A lattice model study of the requirements for folding to the native state. J. Mol. Biol. 235:1614-1636, 1994.

[22] Shakhnovich, E., Gutin, A.M. Formation of unique structure in polypeptide chains. Theoretical investigation with the aid of a replica approach. Biophys. Chem. 34:187-199, 1989.

[23] Shakhnovich, E., Farztdinov, G., Gutin, A.M., Karplus, M. Protein folding bottlenecks: A lattice Monte Carlo simulation. Phys. Rev. Lett. 67:1665-1668, 1991.

[24] Skolnick, J., Kolinski, A. Simulation of the folding of a globular protein. Science 250:1121-1125, 1990.

[25] Skolnick, J., Kolinski, A. Dynamic Monte Carlo simulations of a new lattice model of globular protein folding, structure, and dynamics. J. Mol. Biol. 221:499-531, 1991.

[26] Zwanzig, R. Simple model of protein folding kinetics. Proc. Natl. Acad. Sci. 92:9801-9804, 1995.

[27] Zwanzig, R., Szabo, A., Bagchi, B. Levinthal's paradox. Proc. Natl. Acad. Sci. USA 89:20-22, 1992.

[28] Camacho, C.J., Thirumalai, D. Modeling the role of disulfide bonds in protein folding: Entropic barriers and pathways. Proteins Struct. Funct. Genet. 22:27-40, 1995.

[29] Chan, H.S. Kinetics of protein folding. Nature 373:664-665, 1995.

[30] Derrida, B. Random-energy model: Limit of a family of disordered models. Phys. Rev. Lett. 45:79-82, 1980.

[31] Goldstein, R.A., Luthey-Schulten, Z.A., Wolynes, P.G. Optimal protein-folding codes from spin-glass theory. Proc. Natl. Acad. Sci. USA 89:4918-4922, 1992.

[32] Socci, N.D., Onuchic, J.N. Folding kinetics of protein-like heteropolymers. J. Chem. Phys. 101:1519-1528, 1994.

[33] Camacho, C.J., Thirumalai, D. Kinetics and thermodynamics of folding in model proteins. Proc. Natl. Acad. Sci. USA 90:6369-6372, 1993.

[34] Thirumalai, D. From minimal models to real proteins: Time scales for protein folding kinetics. J. Physique (Paris) I 5:1457-1467, 1995.

[35] Shakhnovich, E., Gutin, A.M. Enumeration of all compact conformations of copolymers with random sequence of links. J. Chem. Phys. 93:5967-5971, 1990.

[36] White, S.H., Jacobs, R.E. The evolution of proteins from random amino acid sequences. I. Evidence from the lengthwise distribution of amino acids in modern protein sequences. J. Mol. Evol. 36:79-95, 1993.

[37] Klimov, D.K., Thirumalai, D., 1994 (unpublished).

[38] Garel, T.R., Leibler, L., Orland, H. Random hydrophilic-hydrophobic copolymers. J. Physique (Paris) II 4:2139-2148, 1994.

[39] Miller, R., Danko, C.A., Fasolka, M.J., Balazs, A.C., Chan, H.S., Dill, K.A. Folding kinetics of proteins and copolymers. J. Chem. Phys. 96:768-780, 1992.

[40] Binder, K.A. Theory and technical aspects of Monte Carlo simulations. In: "Monte Carlo methods in statistical physics". Binder, K.A., (ed.). Berlin, Heidelberg, New York, Tokyo: Springer Verlag. 1986:26-30.

[41] Chan, H.S., Dill, K.A. The effects of internal constraints on the configurations of chain molecules. J. Chem. Phys. 92:3118-3135, 1990.

[42] Karplus, M., Sali, A. Theoretical studies of protein folding and unfolding. Curr. Opin. Struct. Biology 5:58-73, 1995.

[43] Honeycutt, J.D., Thirumalai, D. The nature of folded states of globular proteins. Biopolymers 32:695-709, 1992.

[44] Guo, Z., Thirumalai, D. Kinetics of protein folding: Nucleation mechanism, time scales, and pathways. Biopolymers 36:83-103, 1995.

[45] Martin, J.L. Computer enumerations. In: "Phase transitions and critical phenomena".

Domb, C., Green, M.S. (eds.). New York: Academic Press, 1974:102.

[46] Shakhnovich, E., Gutin, A.M. A new approach to the design of stable proteins. Protein Eng. 6:793-800, 1993.

[47] Shakhnovich, E. Proteins with selected sequences fold into unique native conformation. Phys. Rev. Lett. 72:3907-3910, 1994.

[48] Mountain, R.D., Thirumalai, D. Quantitative measure of efficiency of Monte Carlo simulations. Physica A 210:453-460, 1994.

[49] Karplus, M., Sali, A., Shakhnovich, E. Kinetics of protein folding. Nature 373:665, 1995.

[50] Thirumalai, D., Guo, Z. Nucleation mechanism for protein folding and theoretical predictions for hydrogen-exchange labeling experiments. Biopolymers 35:137-140, 1995.

[51] Abkevich, V.I., Gutin, A.M., Shakhnovich, E. Specific nucleus as the transition state for protein folding: Evidence from the lattice model. Biochemistry 33:10026-10036, 1994.

[52] Abkevich, V.I., Gutin, A.M., Shakhnovich, E. Free energy landscape of protein folding kinetics: Intermediates, traps, and multiple pathways in theory and lattice model simulations. J. Chem. Phys. 101:6052-6062, 1994.

[53] Otzen, D.E., Itzhaki, L.S., Fersht, A.R. Structure of the transition state for the folding/unfolding of the barley chymotrypsin inhibitor 2 and its implications for mechanisms of protein folding. Proc. Natl. Acad. Sci. 91:10422-10425, 1994.

[54] Betancourt, M.R., Onuchic, J.N. Kinetics of protein-like models: The energy landscape factors that determine folding. J. Chem. Phys. 103:773-787, 1995.

[55] Socci, N.D., Onuchic, J.N. Kinetic and thermodynamic analysis of protein-like heteropolymers: Monte Carlo histogram technique. J. Chem. Phys. 103:4732-4744, 1995.

[56] Bai, Y, Sosnick, T.R., Mayne, L., Englander, S.W. Protein folding intermediates: Native-state hydrogen exchange. Science 269:192-197, 1995.

[57] Fersht, A.R. Optimization of rates of protein folding: The nucleation - condensation mechanism and its implications. Proc. Natl. Acad. Sci. 92:10869-10873, 1995.

[58] Guo, Z., Thirumalai, D. Kinetics and thermodynamics of folding of a four-helix bundle protein (unpublished).

FIGURES

Fig. 1. Native structures for two sequences with $N = 15, B_0 = -0.1$. These structures are the lowest energy structures obtained by full enumeration of all the possible conformations. (a) This corresponds to a sequence for which the lowest energy structure displayed is fully compact. It contains 11 topological contacts which are ternary interactions between between two beads that are separated by at least two other beads along the backbone. (b) An example of the lowest energy non-compact structure containing only 10 topological contacts. In both cases the native state is non-degenerate. Such contacts between non-bonded residues are shown as dashed lines.

Fig. 2. Representation of the native structures for two sequences with $N = 27, B_0 = -0.1$. The native structures were determined by a combination of slow cooling procedure and standard Monte Carlo algorithm. The details are given in Appendix A. (a) For this sequence the native structure is fully compact and contains 28 topological contacts. (b) An example of the native structure that is non-compact containing 22 topological contacts. Such contacts between non-bonded residues are shown as dashed lines.

Fig. 3. Lower part of the energy spectrum for ten sequences. The value of $N = 15$ and $B_0 = -0.1$. The spectra were obtained by explicitly enumerating all the possible conformations of the chain for each sequence. The value of the energy gap separating the two lowest energy levels and the number of the sequence in the database are given below each spectrum.

Fig. 4. Lower part of energy spectra for 10 optimized sequences ($N = 27, B_0 = -0.1$) labeled 61 through 70. The left columns of each sequence are the energy levels obtained from slow cooling Monte Carlo simulations. The columns on the right represent the energy spectra of compact structures. Below each pair of spectrum columns the energy gap Δ calculated from Monte Carlo simulations (upper quantity) and Δ_{CS} calculated from the spectra of compact structures (lower quantity) are indicated. It is seen that for several sequences even the lowest energy in the spectrum of compact structures belongs to continuous part of the "true" spectrum. These spectra clearly show that in general non-compact structures are crucial for the thermodynamics (and kinetics). It is also obvious that $\Delta_{CS} \geq \Delta$ for the sequences with the native conformation being compact structure. This should be true for such sequences in this model for all N and all negative values of B_0.

Fig. 5. The set of moves used in the Monte Carlo simulations: (i) Corner flip; (ii) Crankshaft rotation; (iii) Rotation of end residue.

Fig. 6. Temperature dependence of thermodynamic quantities for sequence 14 ($N = 15, B_0 = -0.1$) calculated using full enumeration of all conformations: (a) overlap function $< \chi > (T)$; (b) fluctuations in overlap function $\Delta\chi(T)$; (c) function $< Q > (T)$; (d) specific heat C_v. The peaks in the graphs of $\Delta\chi$ and C_v correspond to the folding transition and collapse temperatures, T_f, T_θ, respectively.

Fig. 7. (a) Dependence of the simulation temperature T_s determined using Eq. (11) on the parameter $\sigma = (T_\theta - T_f)/T_\theta$. T_θ and T_f are calculated from the temperature dependence of C_v and $\Delta\chi(T)$, respectively. (b) Variation of T_s with the energy gap Δ between the ground state and the first excited state for 32 sequences. The energy gap is determined from full enumeration of all possible conformations and is hence exact. The data are for ($N = 15, B_0 = -0.1$).

Fig. 8. (a) The dependence of $\sigma(=(T_\theta - T_f)/T_\theta)$ on the energy gap Δ for various sequences with $(N = 15, B_0 = -0.1)$. This figure shows that there is no trend between σ and Δ because the determination of σ requires the knowledge of the entire energy spectrum. (b) Plot of σ versus Δ expressed in units of T_s - the simulation temperature. This was done because for any useful purposes Δ has to be measured in dimensionless form. The relevant energy is $k_B T_s$. The parameter B (see Eq. (2)) sets the energy scale in terms of which everything is measured. This figure shows even more dramatically the lack of correlation between σ and Δ.

Fig. 9. The upper panel (a) shows the overlap function $< \chi >$ (Eq. (5)) as a function of temperature for the sequence labeled 10 with $N = 15, B_0 = -0.1$. The solid line is obtained by calculating $< \chi >$ using the enumeration of all conformations and the dotted line is the plot of $< \chi >$ calculated using only the set of compact structures. The dashed line is given by the constant value of $< \chi >= 0.21$. The intersection of the solid line with the dashed line determines the simulation temperature, T_s. The constant value of $< \chi >= 0.21$ is chosen so that $T_s < T_f$ for all sequences. The lower panel displays the temperature dependence of $\Delta\chi$. As in Fig. (9a) the solid line is the exact result obtained by full enumeration while the dotted line is the corresponding result for $\Delta\chi$ using compact structures only. Note that the folding temperature T_f obtained from the peak of the solid line is considerably lower than the peak in the dotted line. For all the sequences examined T_f is also less than the midpoint of $< \chi >$ or $< Q >$ (see Fig. (6c)).

Fig. 10. Same as Fig. (9) except the curves are for a sequence labeled 91 which has $N = 15, B_0 = -2.0$. In this case Fig. (10b) shows that the difference in T_f (i.e., between the peaks in the solid curve (full enumeration) and the dotted curve (compact structures only)) is less than for the case with $B_0 = -0.1$.

Fig. 11. Dependence of the folding time τ_f on $\sigma = (T_\theta - T_f)/T_\theta$ for a number of sequences all with $N = 15$. The folding time for each sequence is obtained by fitting $< \chi(t) >$ to an appropriate number of exponential functions as described in Sec. (II.G). The full circles correspond to $B_0 = -0.1$ while the empty circles are for $B_0 = -2.0$. There are 32 sequences with $B_0 = -0.1$ and 9 sequences with $B_0 = -2.0$. The trend from both these parameter values is clear. The smaller values of σ have smaller folding times. The folding times decreases by nearly five orders of magnitude upon reducing σ from 0.8 to around 0.1. For the same range of σ the folding time is considerably greater for $B_0 = -2.0$ than for $B_0 = -0.1$.

Fig. 12. Dependence of the folding time τ_f on the gap Δ which is the difference in energy between the native conformation and the first excited state. The database of sequences is exactly the same as that used in Fig. (11). As in Fig. (11) the full circles are for $B_0 = -0.1$ and the empty circles corresponds to $B_0 = -2.0$. This figure shows that there is no useful correlation between τ_f and Δ. For a given folding time τ_f one can engineer sequences spanning a wide range of gap (both quite small and large).

Fig. 13. The kinetic probabilities $P_r(E_k)$ (cf. Eq. (16)) (shown as empty bars) corresponding to the largest probabilities that a state with the energy E_k occurs before the native conformation is reached. The sequences displayed are moderate folders ($0.1 \lesssim \sigma \lesssim 0.6$) and slow folders ($\sigma \gtrsim 0.6$). All the sequences correspond to $N = 15, B_0 = -0.1$. The sequences are arranged in increasing order of folding time. For most of the sequences with relatively large folding times there is a finite probability of visiting an intermediate. The fluctuation probabilities $P_{fl}(E_k)$ (Eq. (17)), which probe the probability that the same kinetic intermediate is visited after the chain reaches the native conformation, are shown under hatched bars. These probabilities show that most slower folding sequences rarely visit the kinetic intermediate after initially reaching the native conformation at least on the maximum time scale of the simulations.

Fig. 14. Plots of various properties of the kinetic intermediates for the 32 sequences with $N = 15, B_0 = -0.1$. The sequences are arranged in order of increasing folding time. (a) Fraction of native contacts in the intermediate. The sequences which fold fast have large fraction of native contacts in the intermediate ($\gtrsim 0.7$) while slow folding sequences have typically less than 50% of native contacts. These are misfolded structures which act as traps thus slowing down the folding process. (b) The value of the overlap function χ_k between the kinetic intermediate and the native conformation for the sequences arranged in order of increasing folding time. Since the structural overlap function is a more microscopic order parameter than Q this plot is more informative than Fig. (14a). The trends basically are the same. Intermediates for fast folding sequences have the smallest value of χ_k (are most native-like) and slow folding sequences have large value of χ_k. (c) Plot of the ratio of the average first passage time to reach the kinetic intermediate τ_k to the mean first passage time τ_{fp} to reach the native conformation. The mean first passage time τ_{fp} is obtained from the fraction of unfolded molecules $P_u(t)$ as $\tau_{fp} = \int_0^\infty P_u(t)dt$. The figure clearly shows that for relatively fast folding sequences the kinetic intermediate which is very native-like is reached on time scales comparable to τ_{fp}. For slow folding sequences the kinetic intermediate, which does not share many features in common with the native conformation, is reached very rapidly. For these sequences the rate determining step is the transition from these structures to the native state.

Fig. 15. (a) The temperature dependence of the structural overlap function for a sequence labeled 61 with $N = 27, B_0 = -0.1$. The results obtained by using the slow cooling Monte Carlo simulations (see Appendix A for details) are shown in squares. The solid line through these squares represents the fit of the simulation data by hyperbolic tangents. The dotted line represents exact calculation of the temperature dependence of $< \chi >$ using only the ensemble of compact structures. The simulation temperature is determined from the intersection of the simulation results with the dashed line with $< \chi >= 0.21$. (b) The fluctuations in the overlap function $\Delta\chi$ as a function of temperature. The squares represent the results from the slow cooling Monte Carlo simulations whereas the dotted line shows the corresponding results obtained using the contributions from the compact structures only. The solid line is a polynomial fit through the simulation data.

Fig. 16. Same as Fig. (15) except it is for a sequence labeled 81 which has $N = 27, B_0 = -2.0$. In this case the compact structures are expected to dominate. Although the results here for the both the temperature dependence of $< \chi >$ and $\Delta\chi$ are closer to the simulation data than for sequence 61 (Fig. (15)) there are significant differences in the estimation of T_s and T_f between the simulation results and those obtained from compact structures enumeration. This trend is seen for all sequences.

Fig. 17. (a) Ratio of simulation temperatures obtained using compact structures only T_s^{CSE} in conjunction of Eq. (11) to that obtained for the entire ensemble of conformations $T_s = T_s^{FE}$ for $N = 15, B_0 = -0.1$ for a variety of sequences. (b) Same as Fig. (17a) except that the simulation temperature $T_s = T_s^{MC}$ is obtained using slow cooling Monte Carlo simulations as described in Appendix A. These figures show that T_s^{CSE} is always greater than T_s and often is much greater than T_s. We have excluded those sequences for which the native conformation is non-compact. The sequences are arranged in order of increasing folding time.

Fig. 18. (a) The time dependence of the overlap function $< \chi(t) >$ for the sequences labeled 69 with $N = 27, B_0 = -0.1$. The simulation temperature is $T_s = 1.07$ and the value of $\sigma \approx 0$. The overlap function has been calculated using Eq. (12) by averaging over 200 initial independent conditions. The solid line is a single exponential fit to the simulation data. In this case the folding appears to be an all-or-none process. (b) Same as (a) except the plot shows $< \chi(t) >$ for the sequences labeled 65. The simulation temperature is $T_s = 0.77$ and the value of $\sigma = 0.075$. The solid line is a biexponential fit to the simulation data. In this case folding appears to be a three stage multipathway process.

Fig. 19. The variation of the folding time τ_f with $\sigma = (T_\theta - T_f)/T_\theta$ for $N = 27, B_0 = -0.1$. There are fifteen sequences for which τ_f has been calculated using the procedure described in Sec. (II.G). The basic trend here is the same as for $N = 15$ (see Fig. (11)). There is a dramatic increase in folding time as σ changes from 0.02 to 0.1. Since all the sequences used were optimized the range of σ examined here is considerably less than for $N = 15$.

Fig. 20. Dependence of the folding time τ_f on the gap Δ for the same set of sequences as in Fig. (19). The gap Δ, which is the energy difference between the native conformation and the first excited state, was calculated using the procedure given in Appendix B. It is clear that as for $N = 15$ (see Fig. (12)) there is no useful correlation between τ_f and Δ.

Fig. 21. Plots of the folding time τ_f as a function of the energy gap Δ divided by the simulation temperature T_s. (a) The solid circles correspond to $B_0 = -0.1$ whereas the open circles are for $B_0 = -2.0$. The value of N is 15. (b) This plot is for $N = 27, B_0 = -0.1$. These figures reaffirm even more emphatically the lack of any relationship between τ_f and the energy gap expressed in suitable dimensionless units.

Fig. 22. Dependence of the folding time τ_f on the energy gap Δ_{CS}. (a) The solid circles correspond to $B_0 = -0.1$ and open circles are for $B_0 = -2.0$. The value of $N = 15$. The database of sequences is the same as in Fig. (11). (b) This is for $N = 27$ and $B_0 = -0.1$. The database of sequences is the same as in Fig. (19). These figures show that the folding times do not correlate with the energy gap even when restricted to the ensemble of compact structures.

Fig. 23. Temperature dependence of η (cf. Eq. (22)) which gives the probability that the chain is not in the native conformation. Notice that the temperature is measured in units of $T/T_{s\eta}$. For sequences with a large enough gaps (i.e. $\Delta/k_B T_s \gg 1$) $\eta(T)$ is only a function of $T/T_{s\eta}$ (see Eq. (24)). This is verified for the sequences labeled 10 and 62 for $T/T_{s\eta} \lesssim 1.5$. The temperature $T_{s\eta}$ is determined from the intersection of $\eta(T)$ with the straight dashed line giving the constant value of $\eta = 0.1$. Thus, at these temperatures the probability of being in the native conformation is 0.9.

Fig. 24. (a) Time dependence of the overlap function $< \chi(t) >$ for the sequence labeled 62 with $N = 15, B_0 = -0.1$. The simulation temperature $T_{s\eta} = 0.47$ was determined using Eq. (22). The equilibrium value of $< \chi >$ from exact enumeration is 0.028 at $T = T_{s\eta}$. At this temperature, at which the probability of the chain being in the native state is 0.9, $< \chi(t) >$ shows a biexponential behavior. This fast folding sequence ($\sigma \approx 0.0$) exhibits an exponential time dependence at $T = T_s = 0.76$. (b) Plot of the fraction of unfolded molecules $P_u(t)$ (see Eq. (13)) as a function of the number of Monte Carlo steps. The solid line is a biexponential fit to the simulation data. At this low temperature a fraction of molecules get trapped in the kinetic intermediate and the transition from this intermediate to the native conformation represents the slow step in the folding process.

Fig. 25. (a) Same as Fig. (24a) except it is for the sequence labeled 10, whose σ is 0.19. This is a moderate folding sequence in our computational scheme. The dashed line corresponds to the equilibrium value of $< \chi >$ at $T = T_{s\eta} = 0.25$. On the time scale of the simulation (3×10^7 MCS) the equilibrium value is not reached. (b) Time dependence of the fraction of unfolded molecules $P_u(t)$. It is clear that $P_u(t)$ has not decayed significantly on the time scale of the simulations. The simulation temperature $T_{s\eta}$ is so low that only 24% of the initial population of molecules has reached the native state on the time scale of 3×10^7 MCS.

Fig. 26. Probability that the native conformation is populated $P(E_0)$ for 32 sequences with $N = 15, B_0 = -0.1$ at the simulation temperatures T_s (cf. Eq. (11)). The sequences are arranged in order of increasing folding time. The probability ranges from about 0.2 to 0.6. It is clear that some of the slow folding sequences make less frequent transitions to other states from the native state whereas the fast folding sequences often visit native-like conformations.

(a)

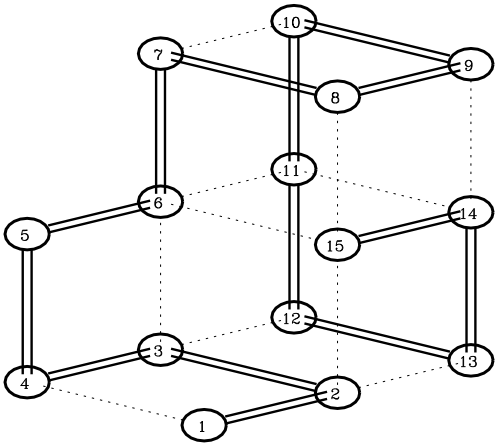

(b)

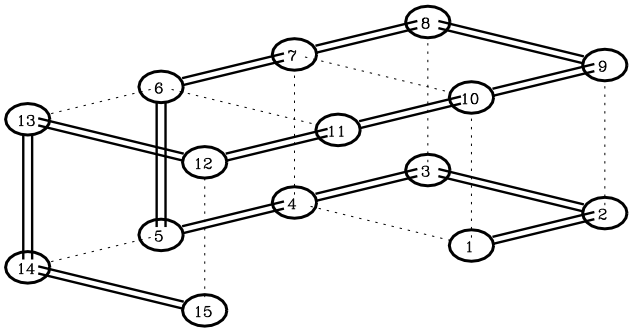

Fig. 1(a,b)

(a)

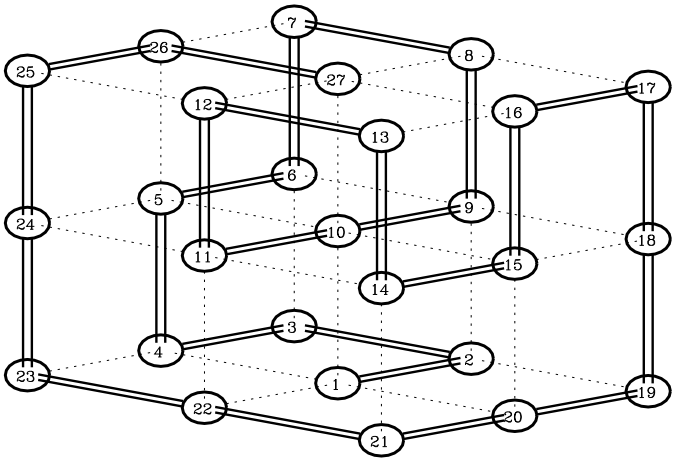
7
26
8
25
27
17
12
16
13
6
5
9
24
10
18
11
15
14
3
4
2
23
1
19
22
20
21

(b)

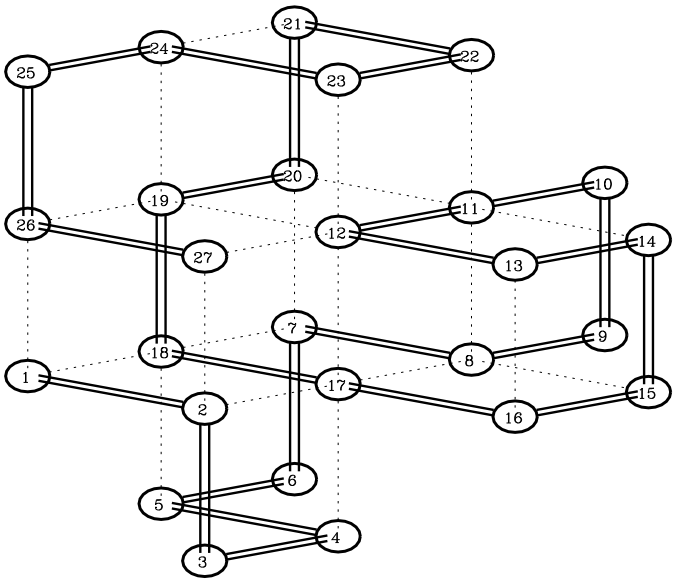
21
24
22
25
23
20
10
19
11
26
12
14
27
13
7
9
18
8
1
17
15
2
16
6
5
4
3

Fig. 2(a,b)

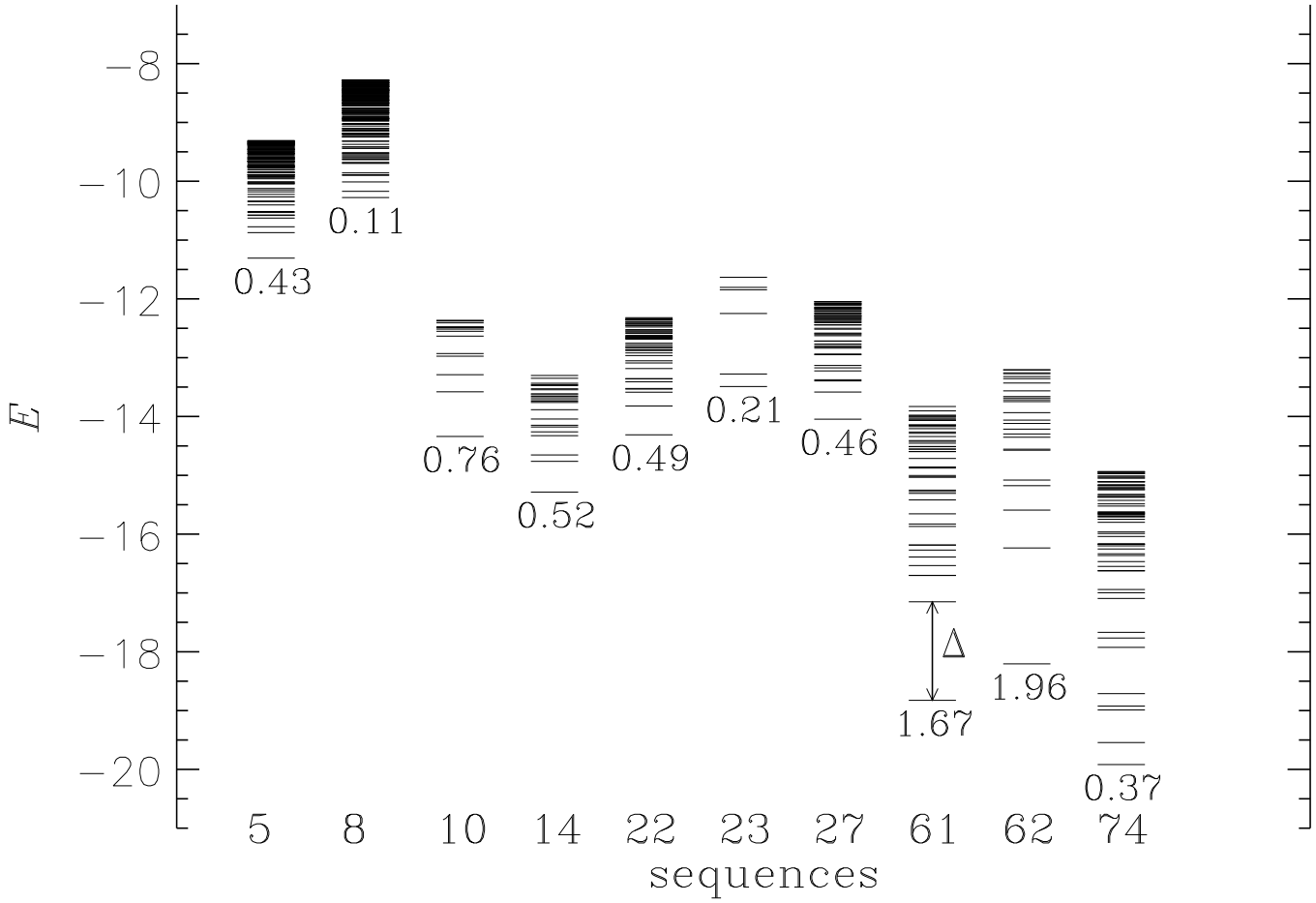
−8
−10
−12
−14
−16
−18
−20
E
0.43
0.11
0.76
0.52
0.49
0.21
0.46
Δ
1.67
1.96
0.37
5
8
10
14
22
23
27
61
62
74
sequences

Fig. 3

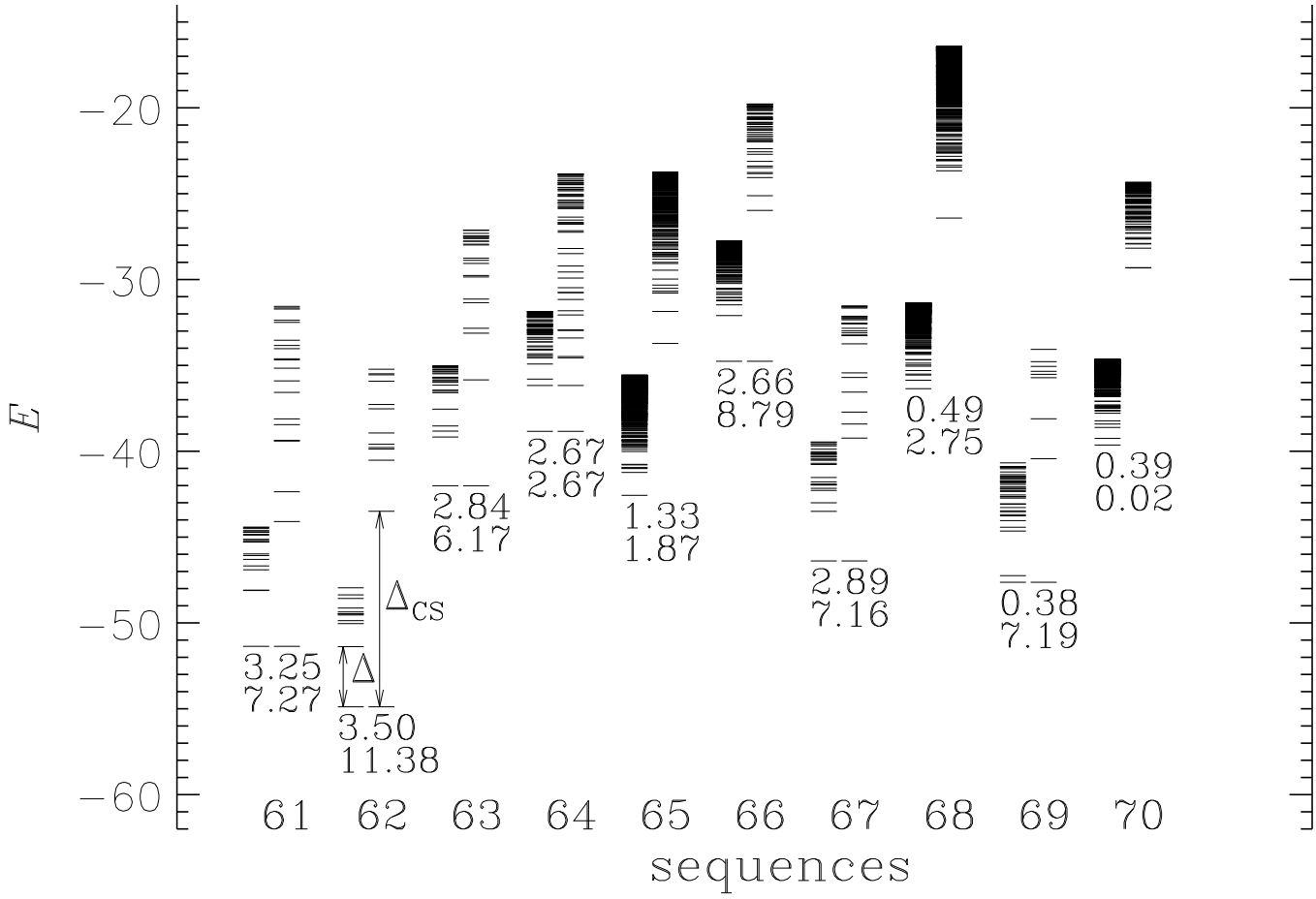
E
−20
−30
−40
−50
−60
61
62
63
64
65
66
67
68
69
70
sequences
3.25
7.27
3.50
11.38
Δ
Δcs
2.84
6.17
2.67
2.67
1.33
1.87
2.66
8.79
2.89
7.16
0.49
2.75
0.38
7.19
0.39
0.02

Fig. 4

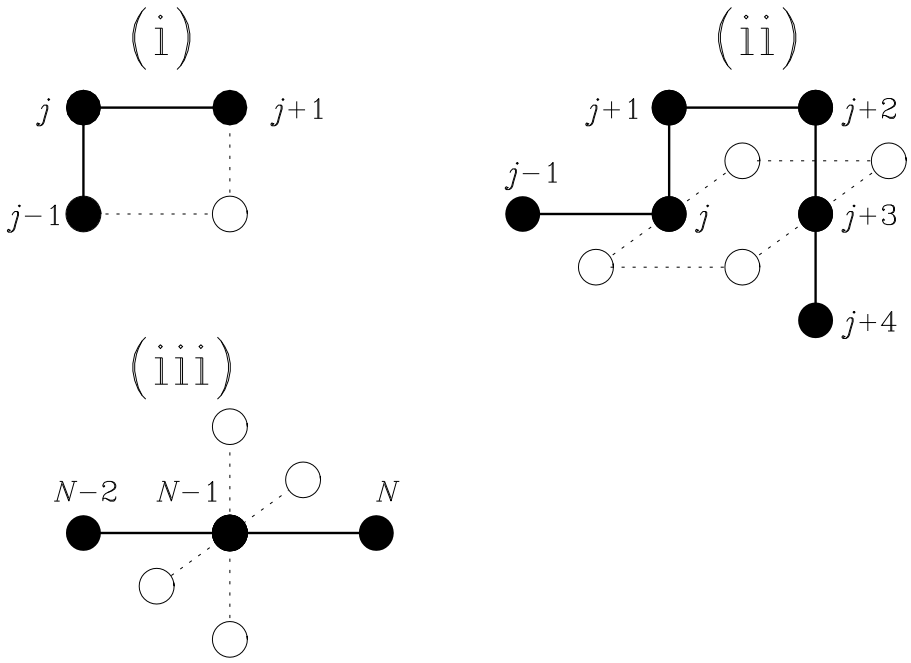

Fig. 5

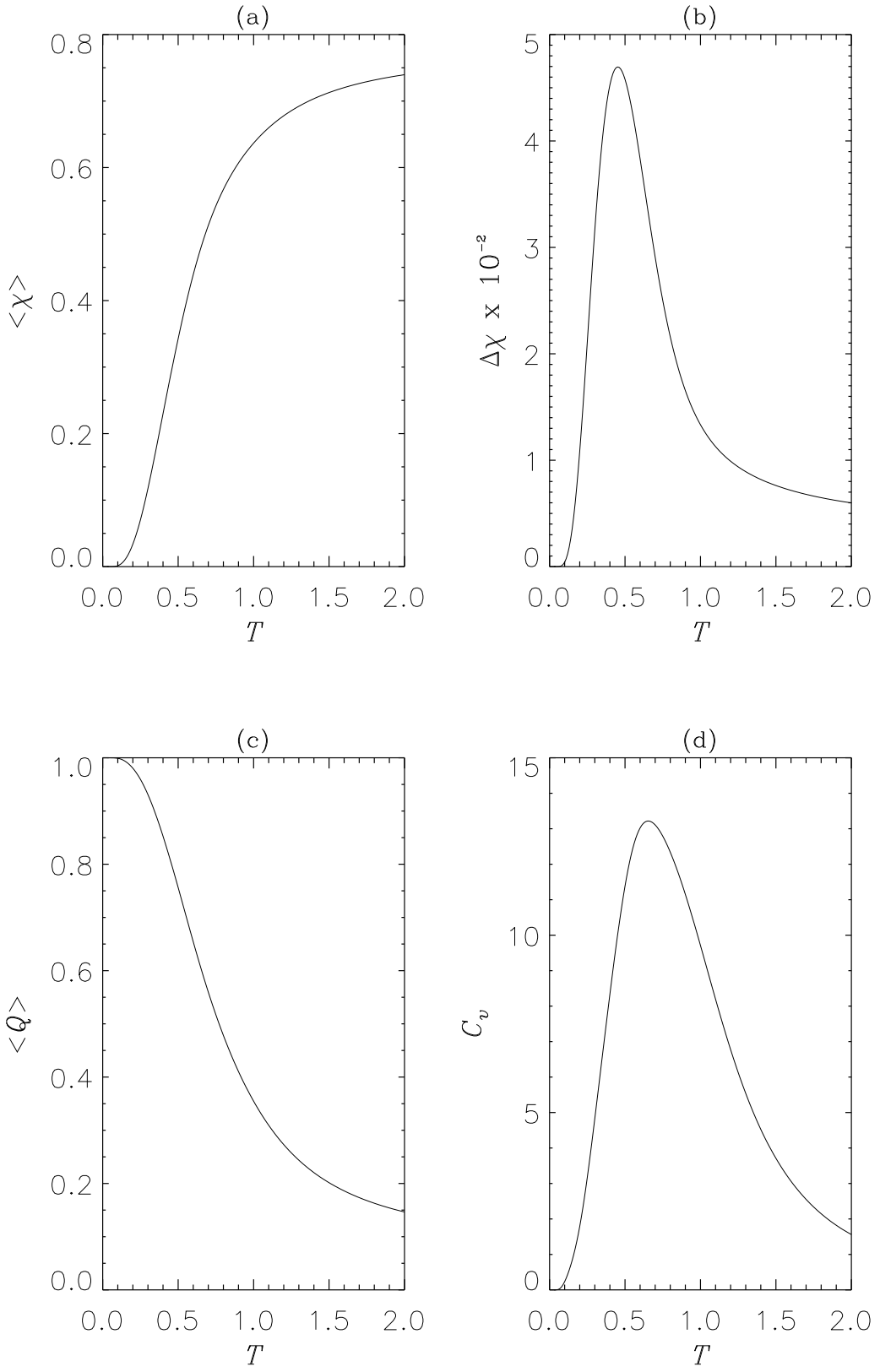
(a)
(b)
(c)
(d)
$\langle\chi\rangle$
$\Delta\chi$ x 10^{-2}
$\langle Q\rangle$
C_v
T
0.0
0.2
0.4
0.6
0.8
1.0
0
1
2
3
4
5
10
15
0.5
1.5

Fig. 6

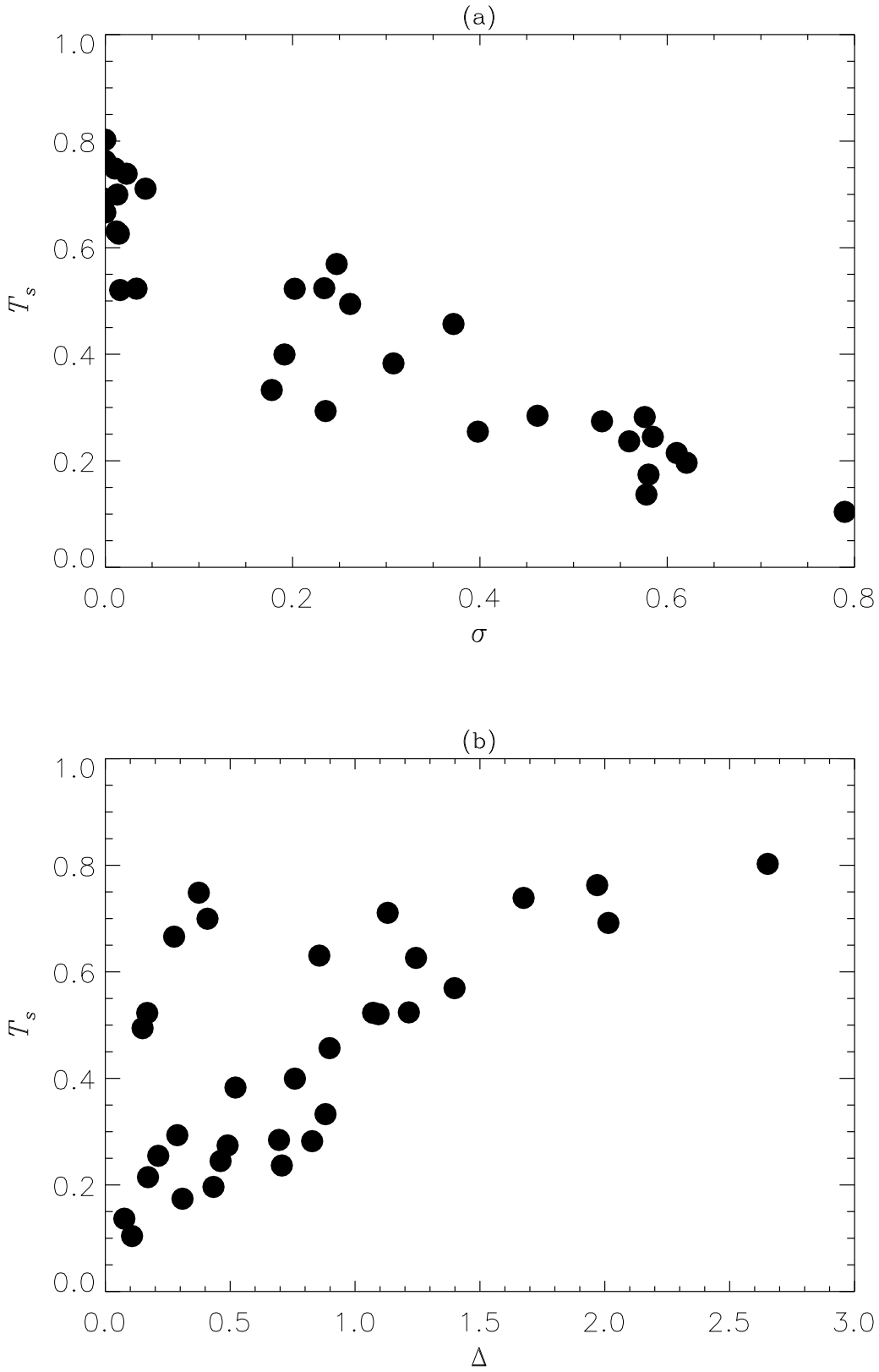
(a)
1.0
0.8
0.6
0.4
0.2
0.0
T_s
0.0
0.2
0.4
0.6
0.8
σ
(b)
1.0
0.8
0.6
0.4
0.2
0.0
T_s
0.0
0.5
1.0
1.5
2.0
2.5
3.0
Δ

Fig. 7

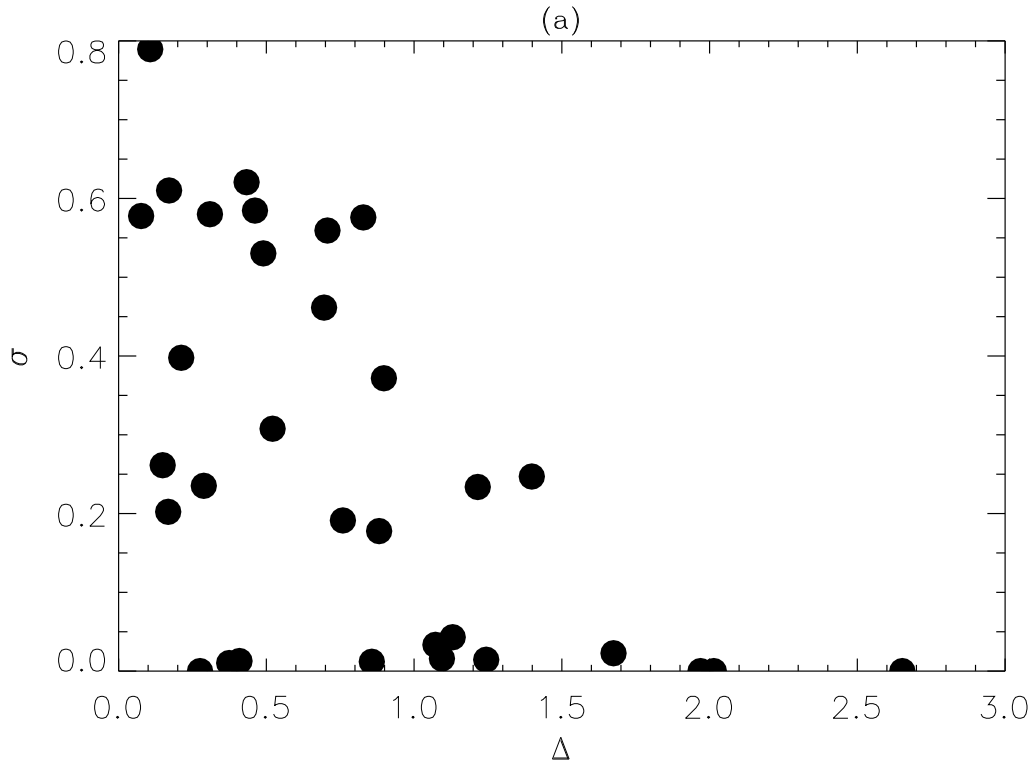

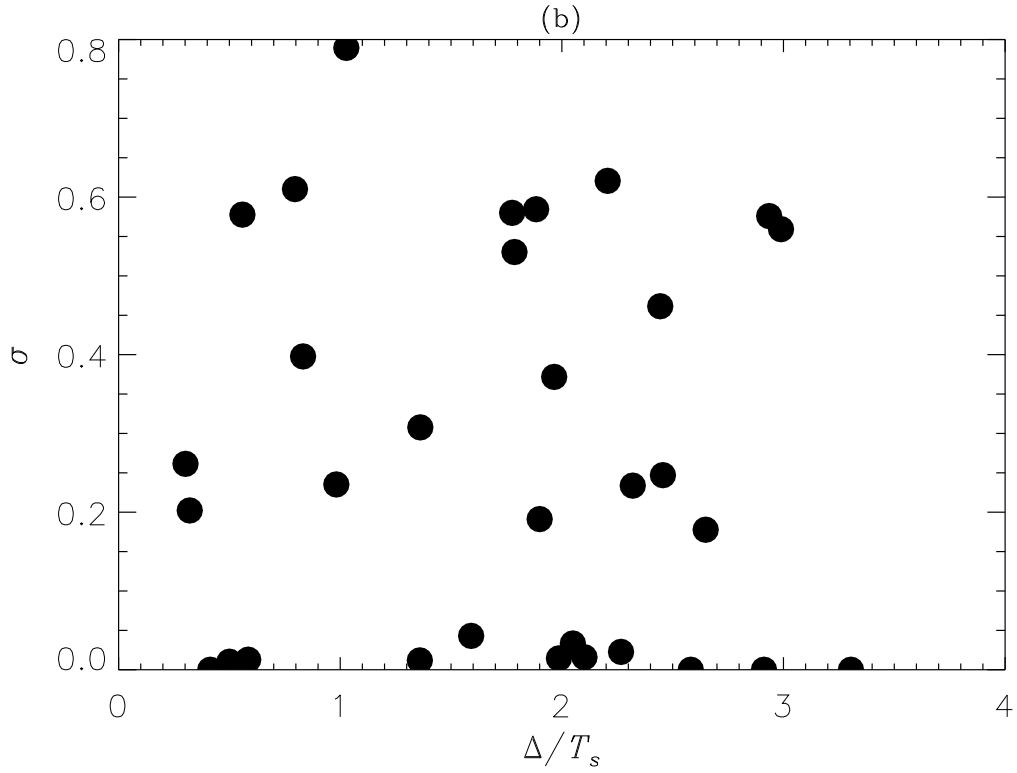

Fig. 8

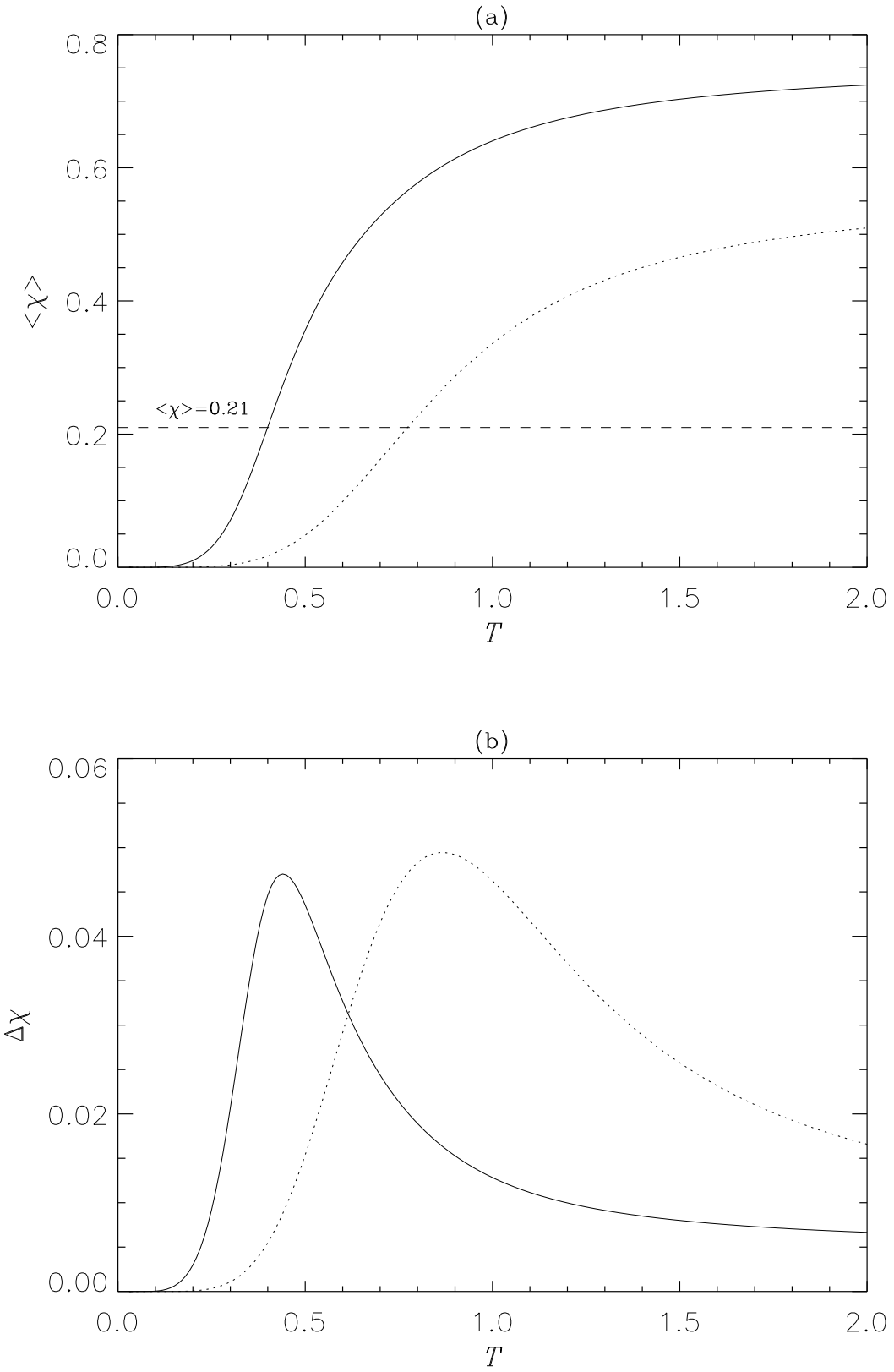
(a)
0.8
0.6
0.4
0.2
0.0
<χ>
<χ>=0.21
0.0
0.5
1.0
1.5
2.0
T
(b)
0.06
0.04
0.02
0.00
Δχ
0.0
0.5
1.0
1.5
2.0
T

Fig. 9

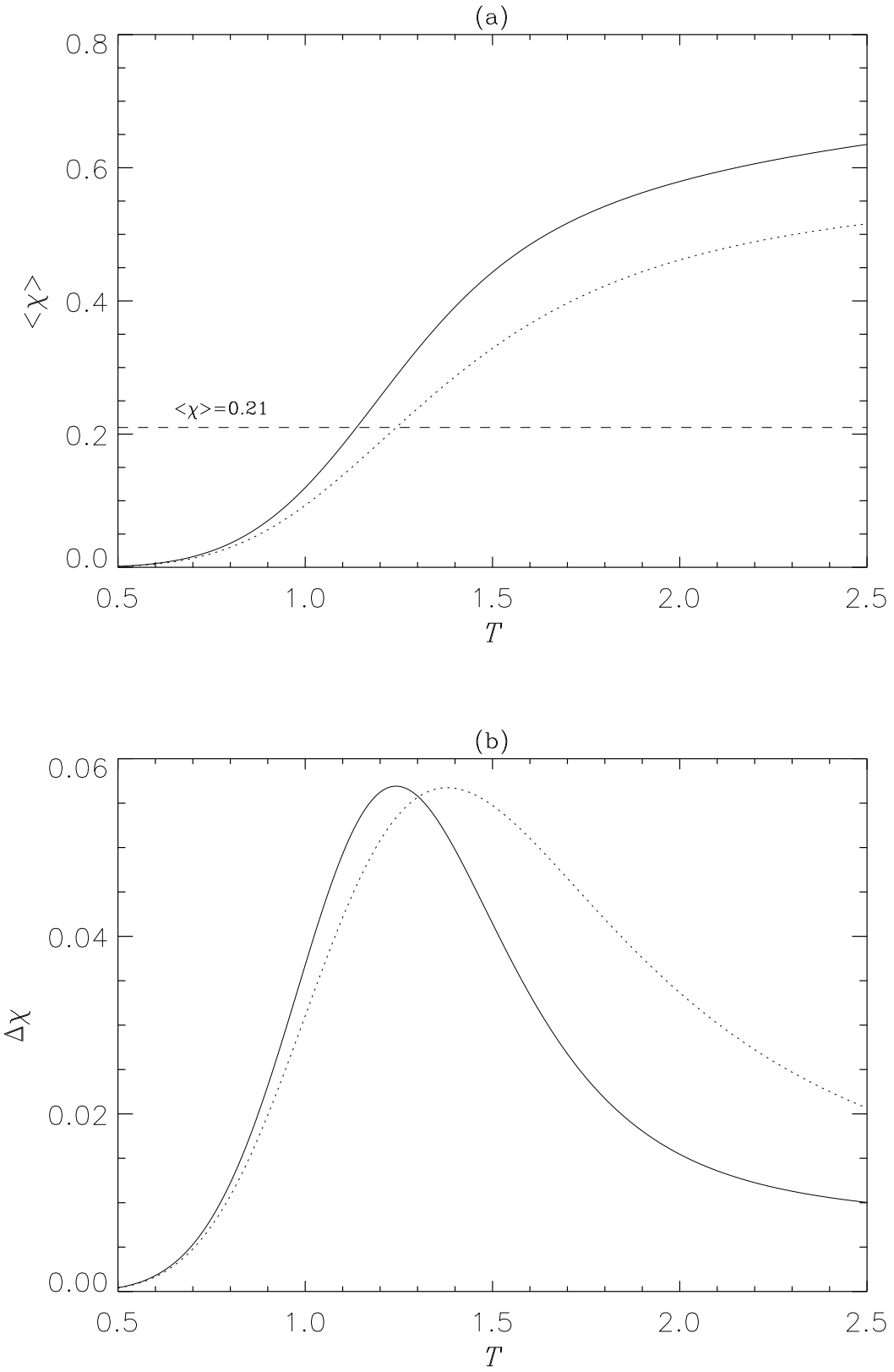
(a)
0.8
0.6
0.4
0.2
0.0
<χ>
<χ>=0.21
0.5
1.0
1.5
2.0
2.5
T
(b)
0.06
0.04
0.02
0.00
Δχ
0.5
1.0
1.5
2.0
2.5
T

Fig. 10

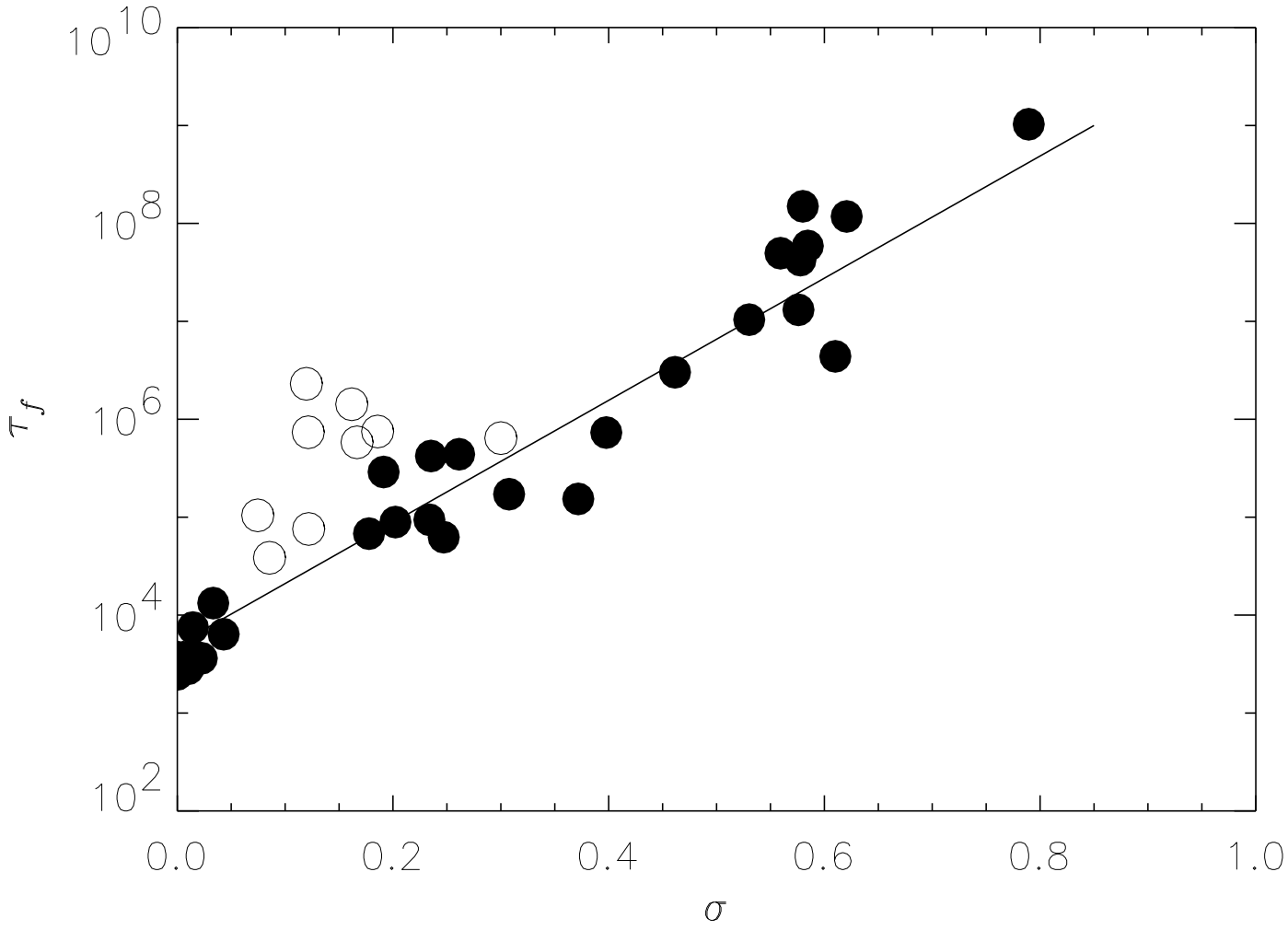

Fig. 11

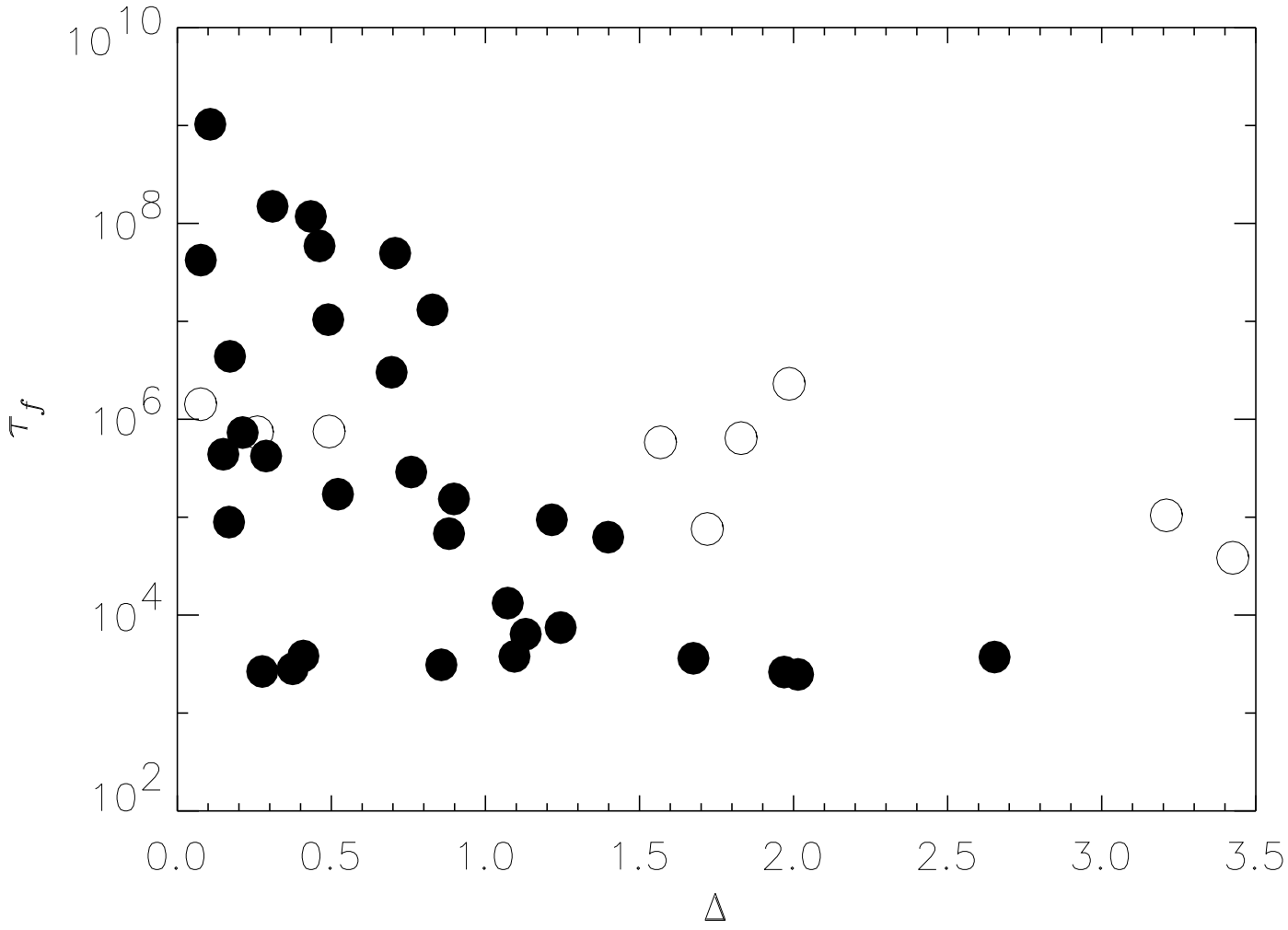

Fig. 12

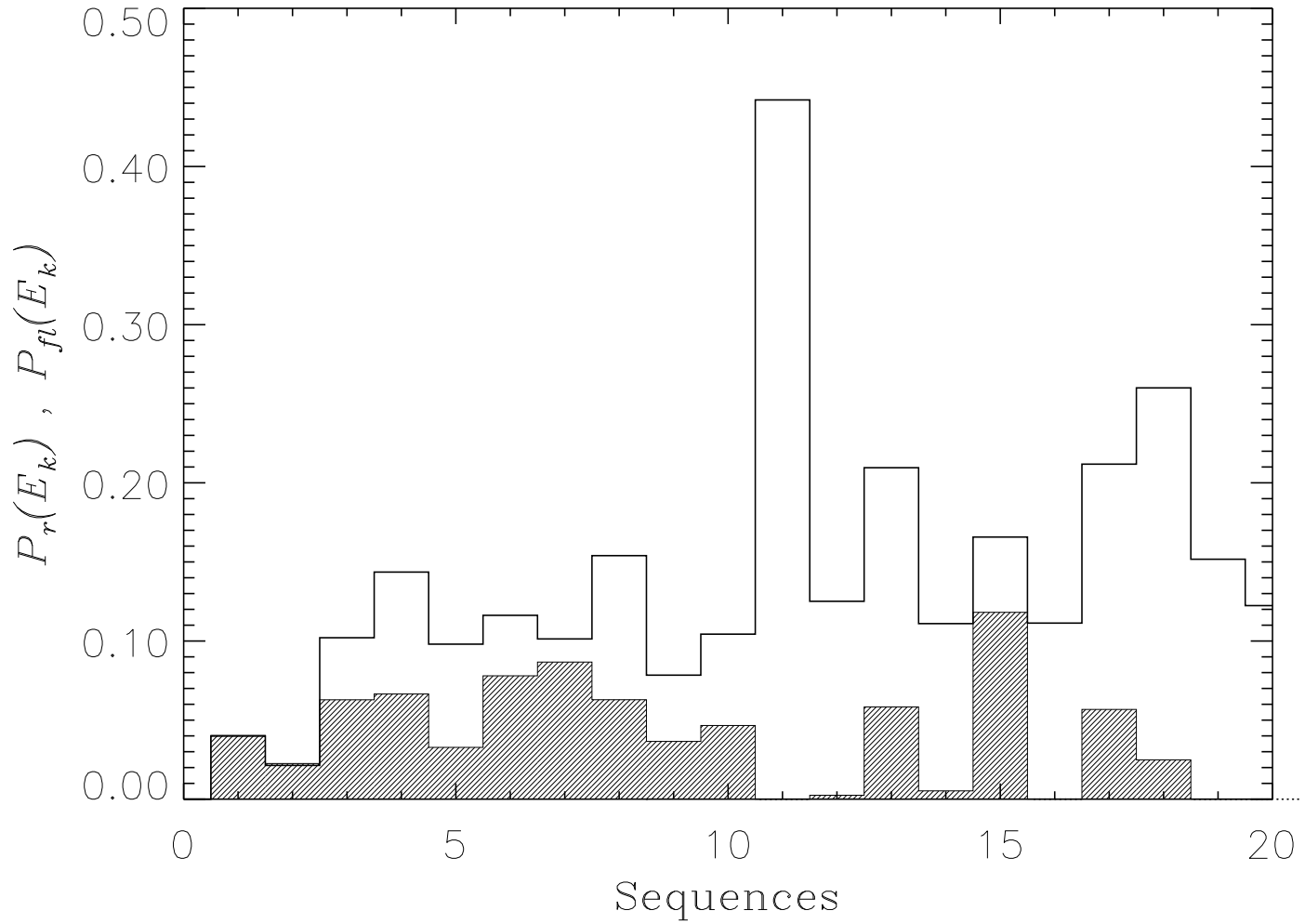

Fig. 13

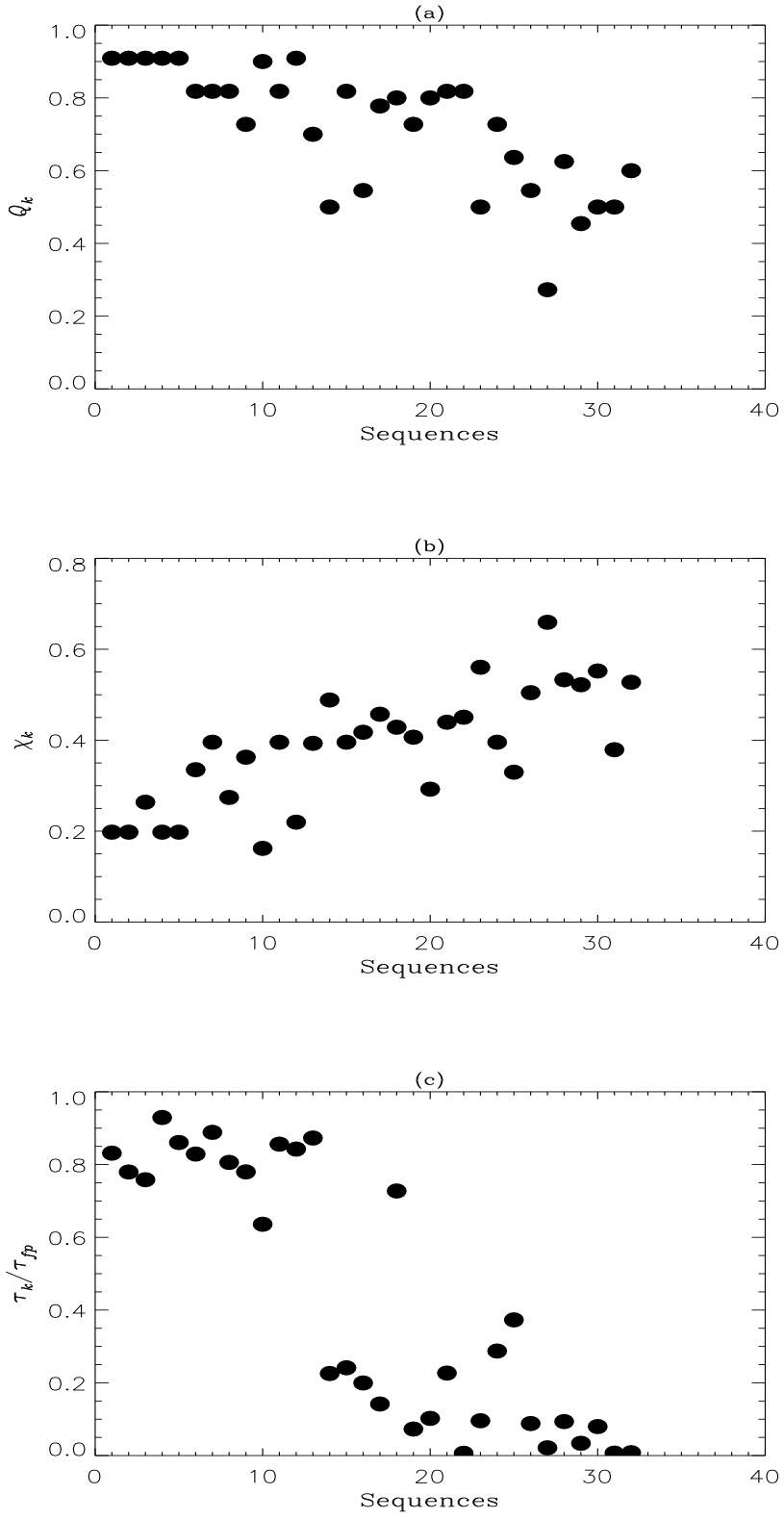

Fig. 14

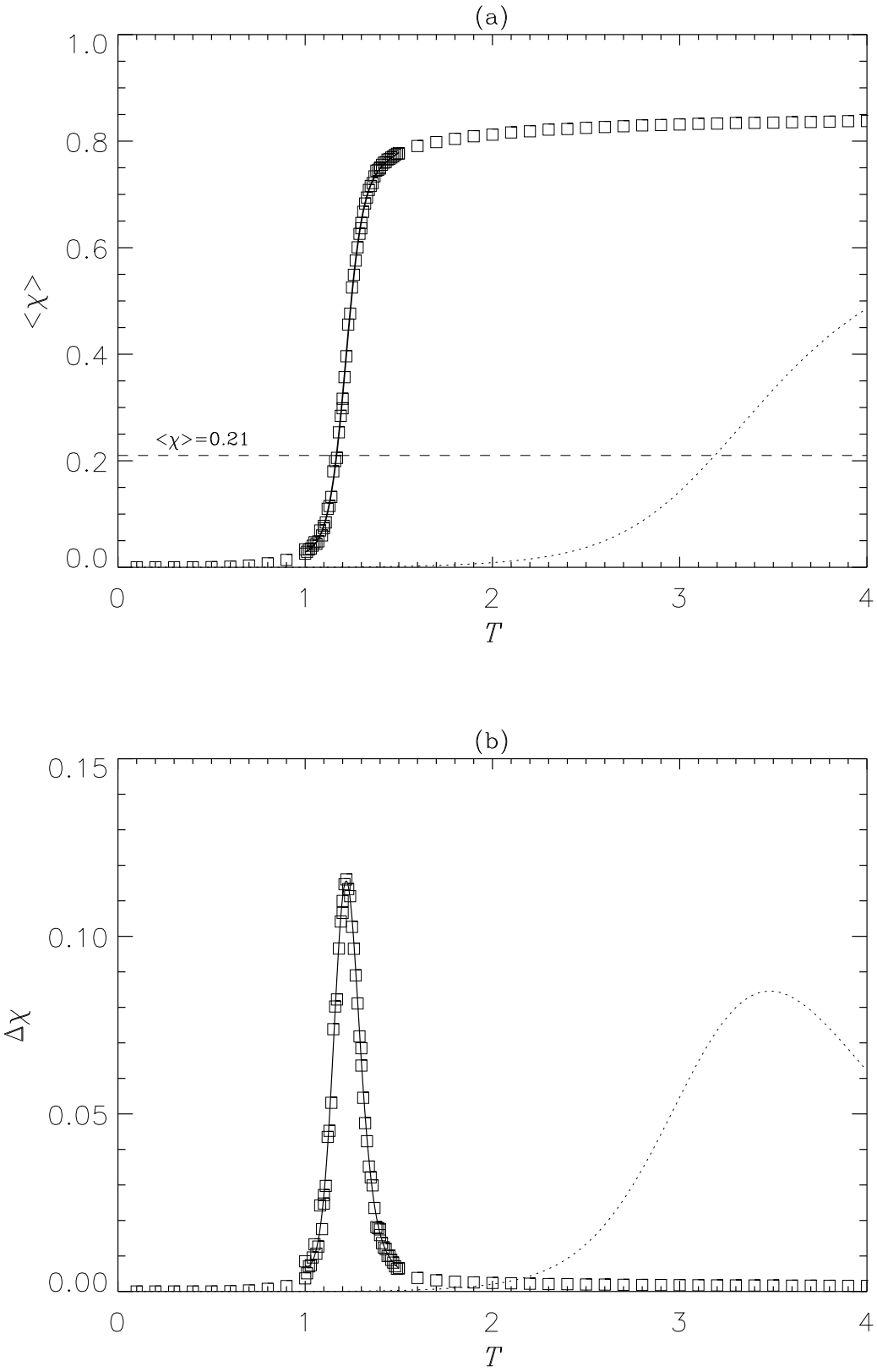

Fig. 15

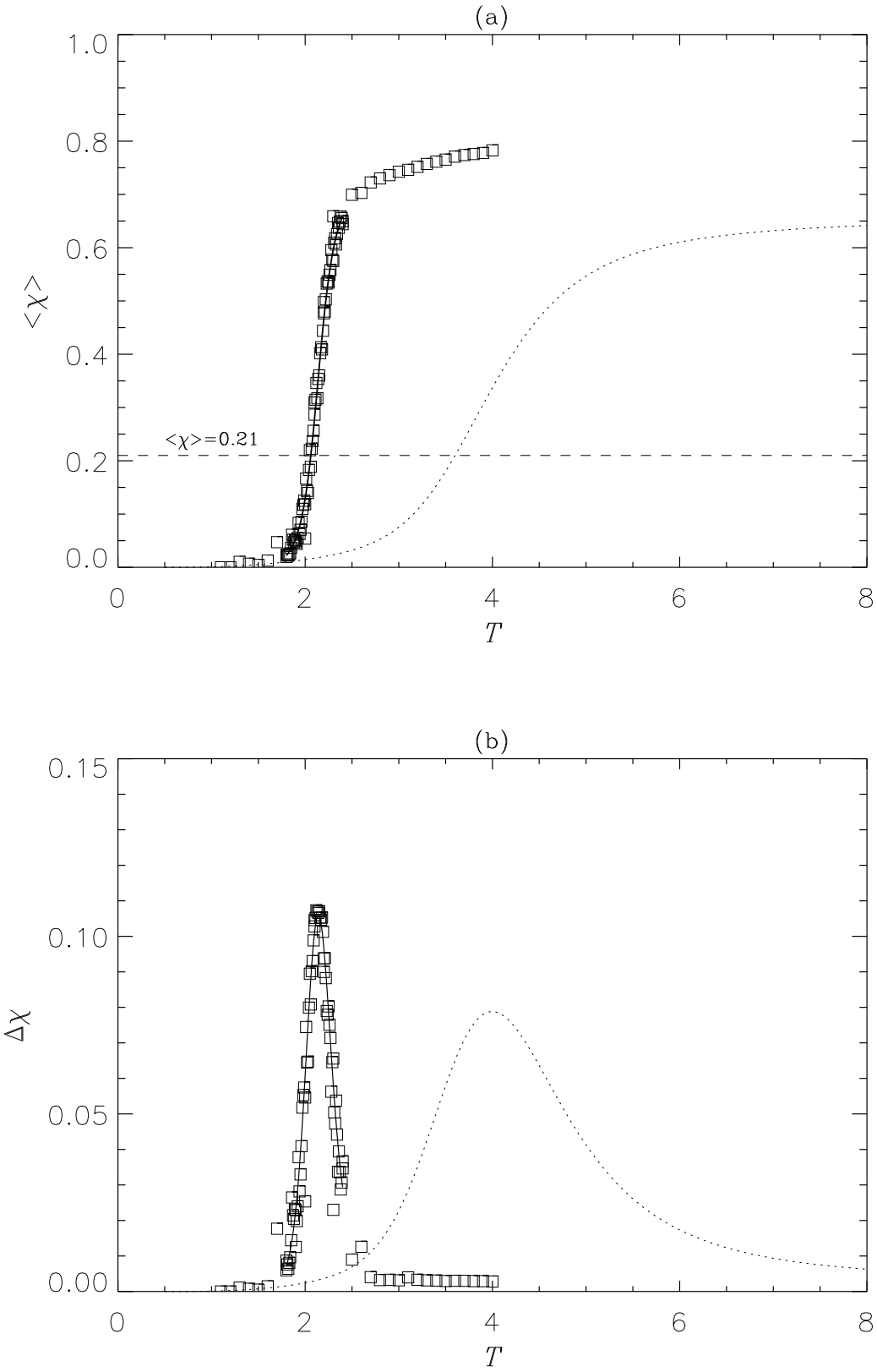

Fig. 16

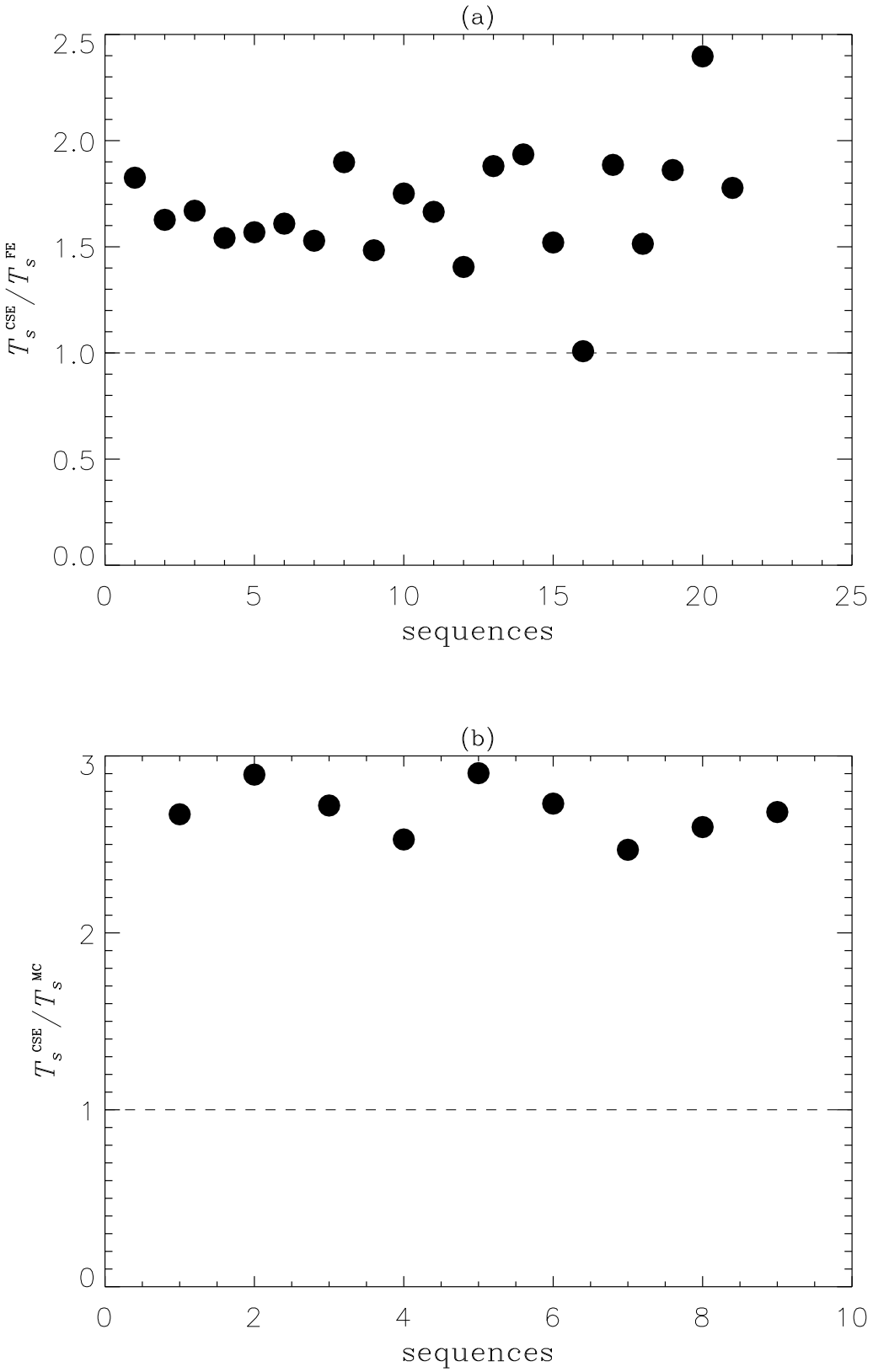
(a)
2.5
2.0
1.5
1.0
0.5
0.0
T_s^{CSE}/T_s^{FE}
0
5
10
15
20
25
sequences
(b)
3
2
1
0
T_s^{CSE}/T_s^{MC}
0
2
4
6
8
10
sequences

Fig. 17

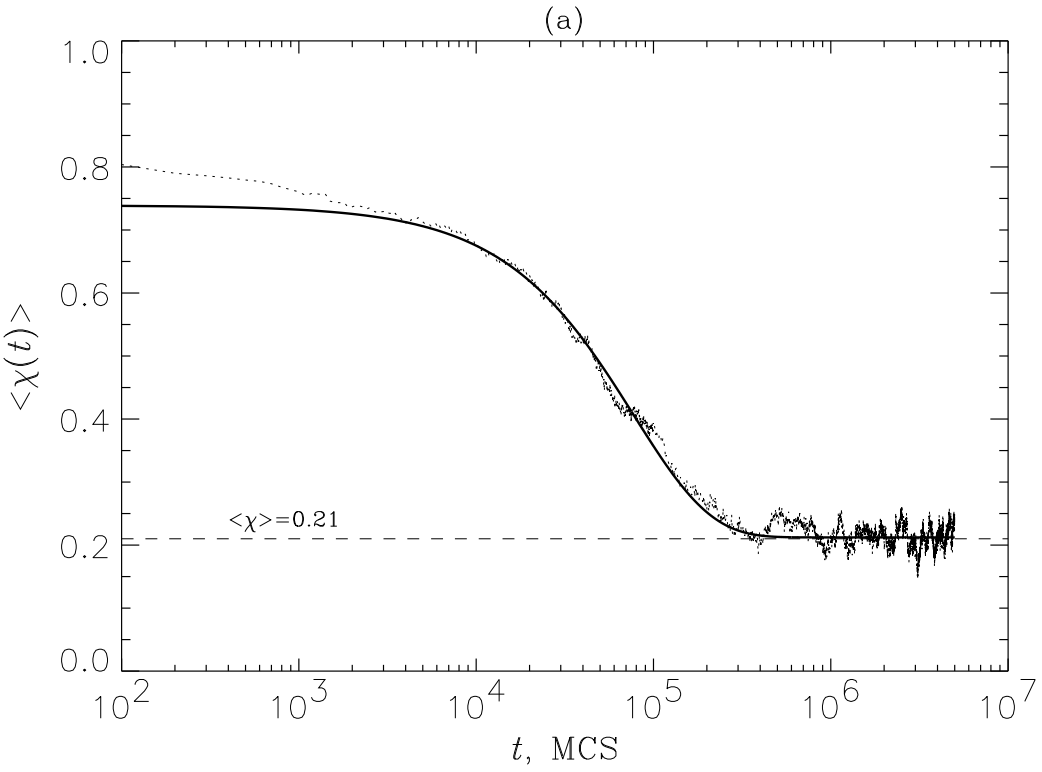
(a)
1.0
0.8
0.6
0.4
0.2
0.0
$<\chi(t)>$
$<\chi>=0.21$
10^2
10^3
10^4
10^5
10^6
10^7
t, MCS

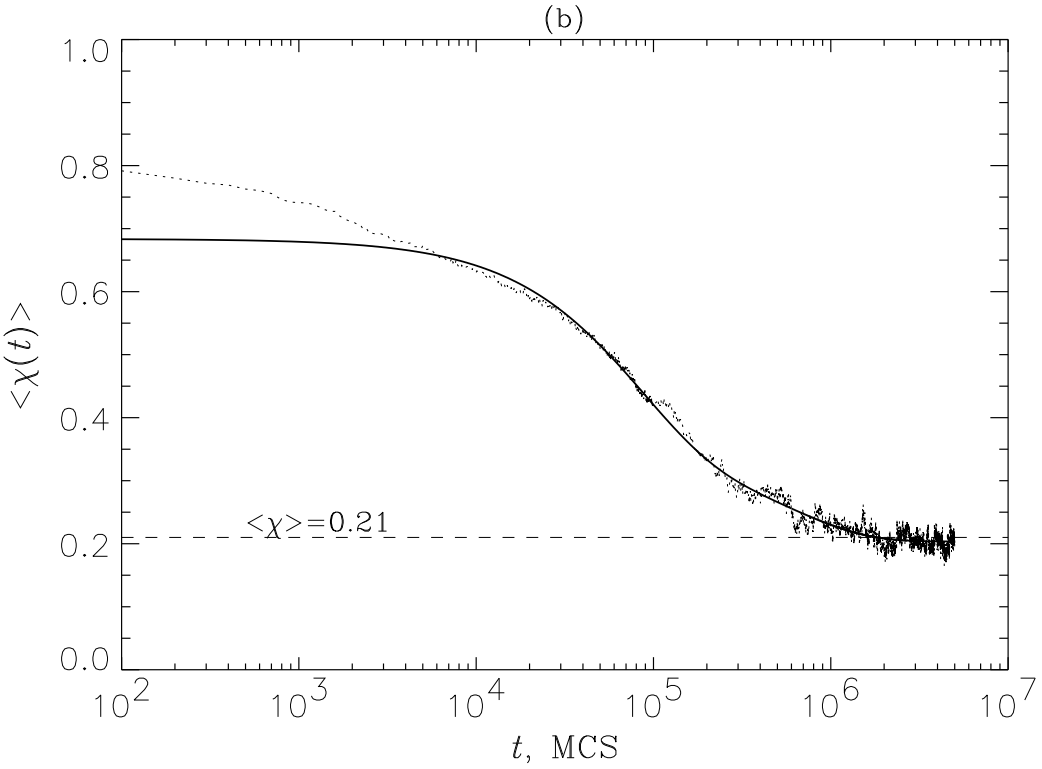
(b)
1.0
0.8
0.6
0.4
0.2
0.0
$<\chi(t)>$
$<\chi>=0.21$
10^2
10^3
10^4
10^5
10^6
10^7
t, MCS

Fig. 18

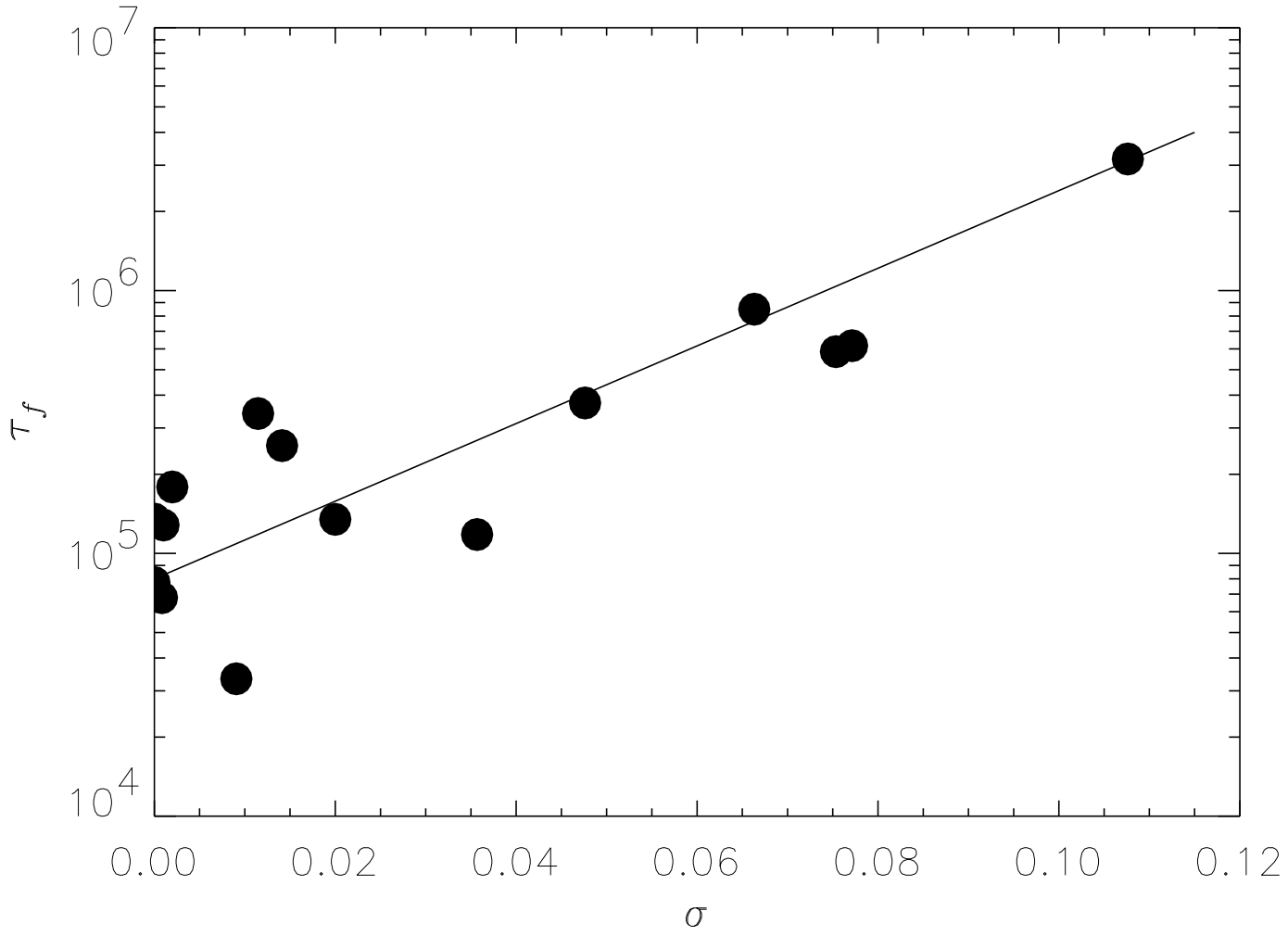

Fig. 19

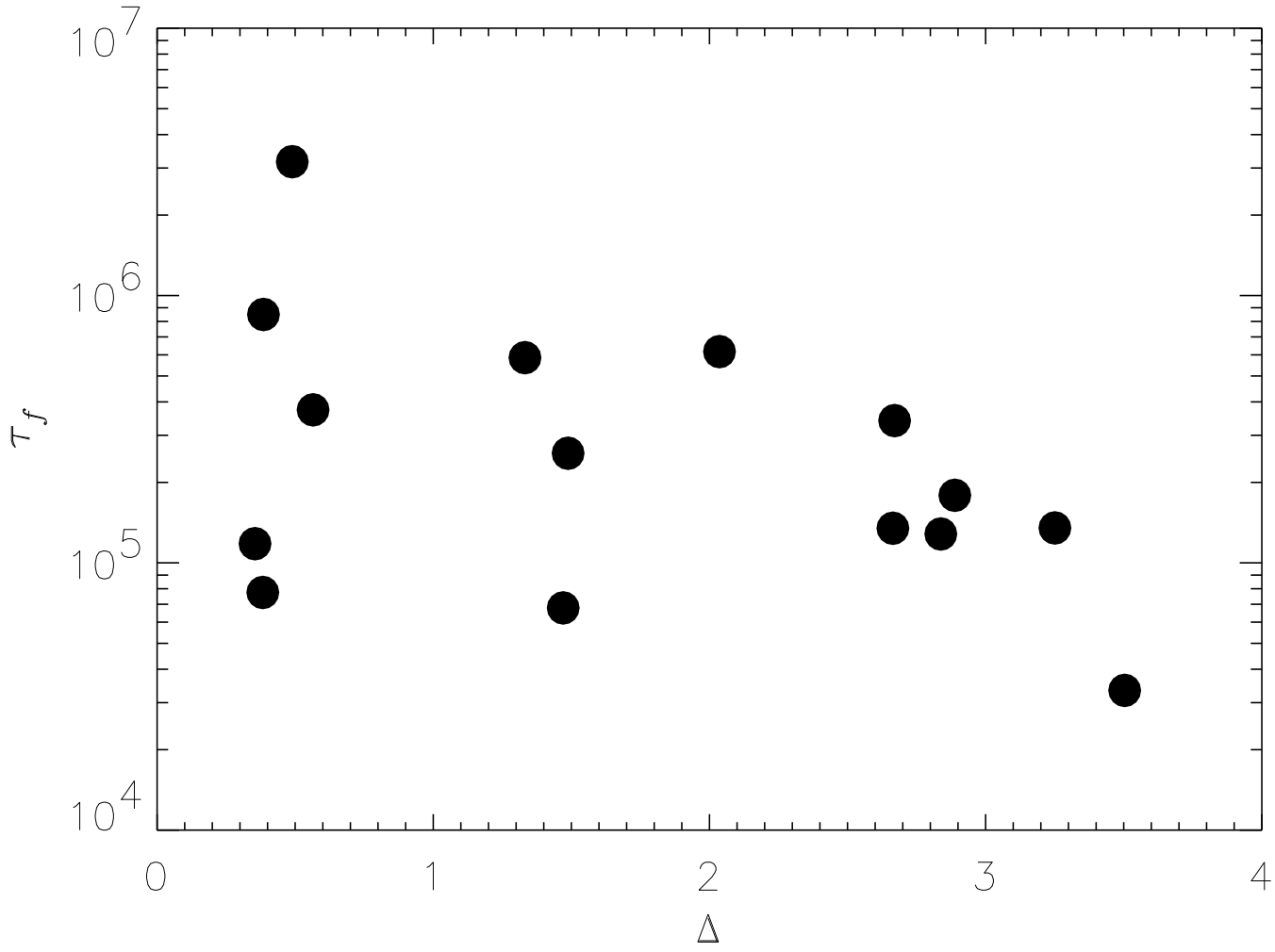

Fig. 20

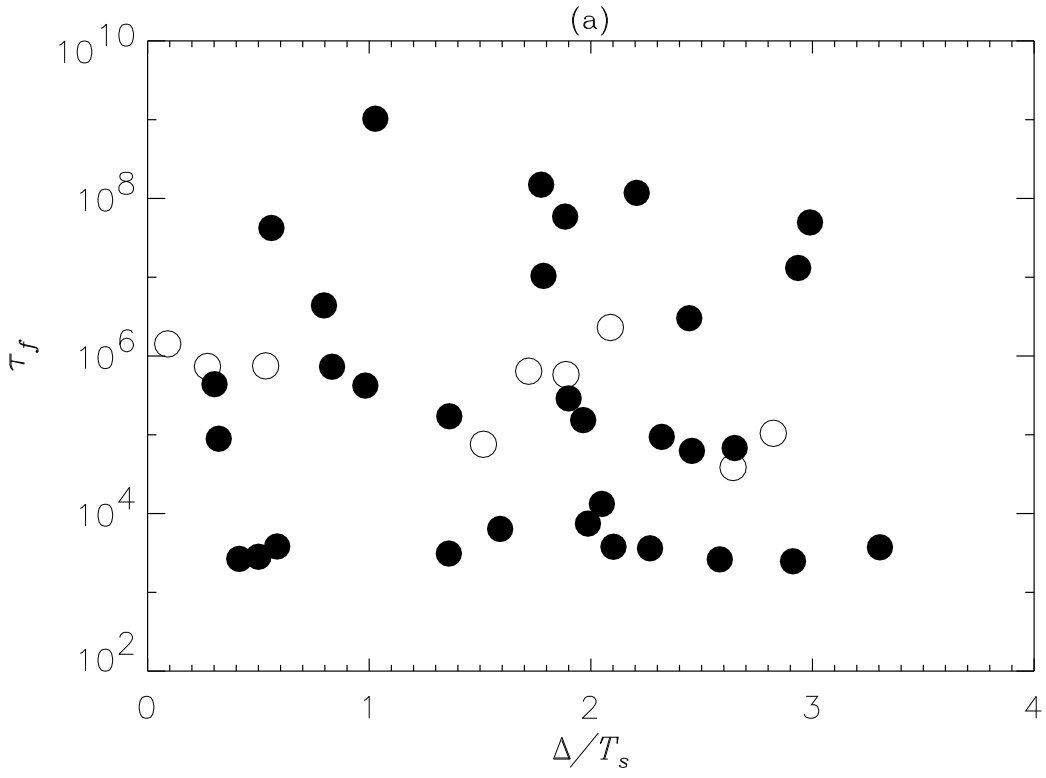
(a)
10^{10}
10^{8}
10^{6}
10^{4}
10^{2}
τ_f
0
1
2
3
4
Δ/T_s

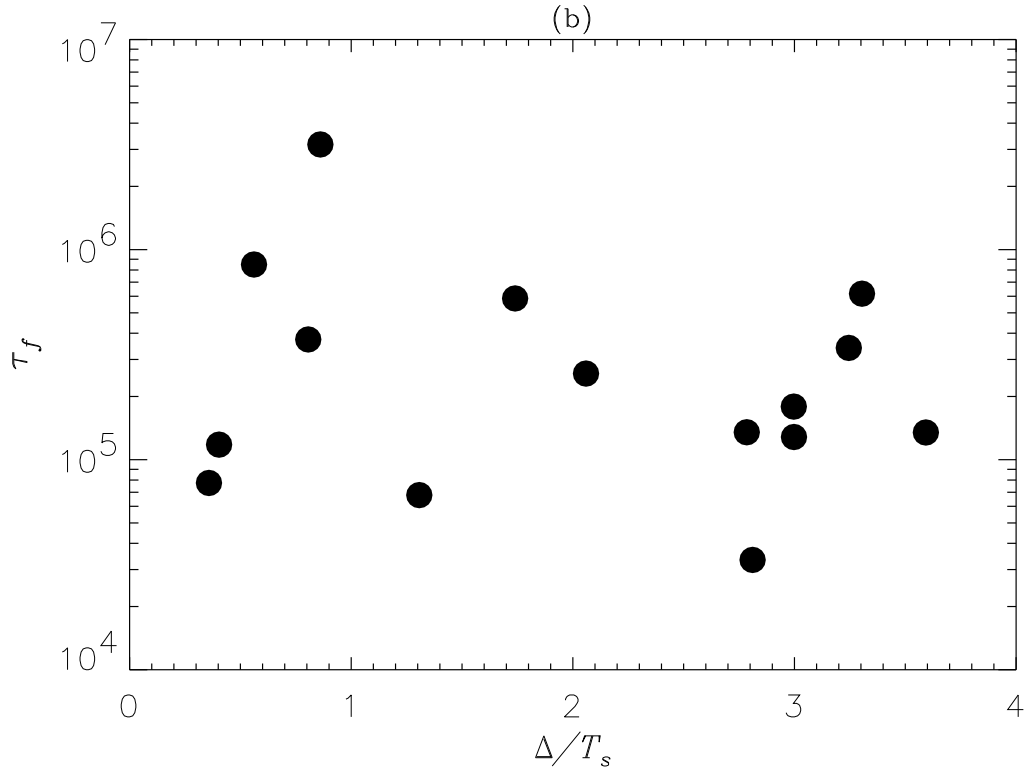
(b)
10^{7}
10^{6}
10^{5}
10^{4}
τ_f
0
1
2
3
4
Δ/T_s

Fig. 21

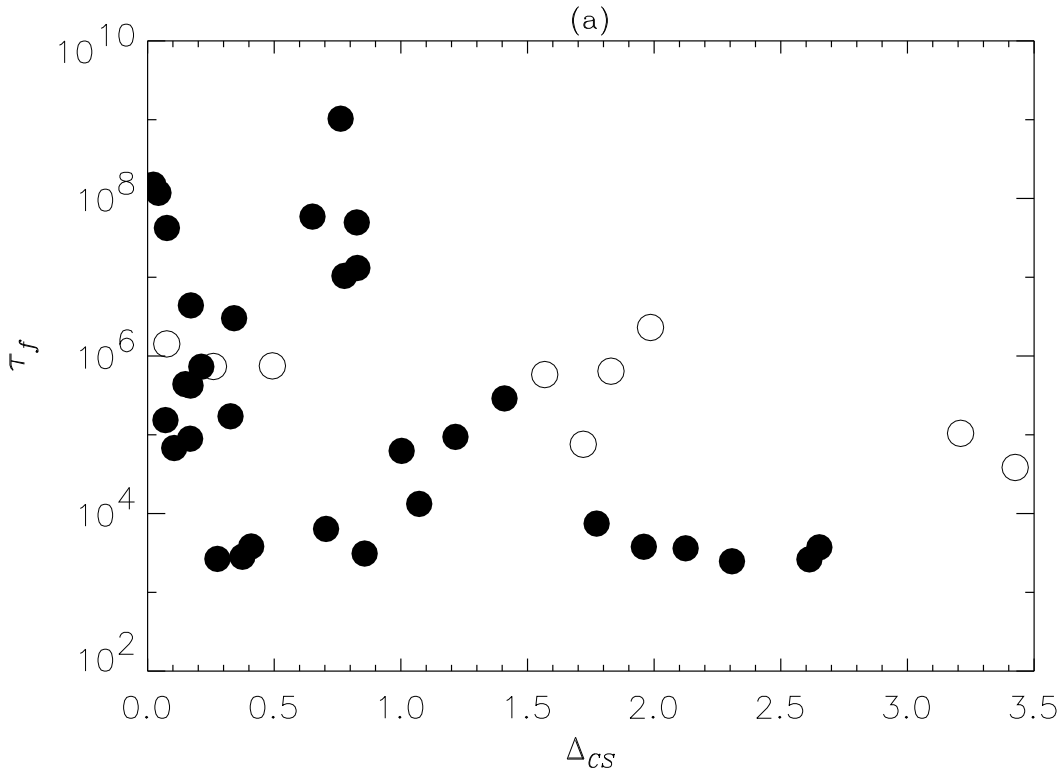
(a)
10^{10}
10^{8}
10^{6}
10^{4}
10^{2}
τ_f
0.0
0.5
1.0
1.5
2.0
2.5
3.0
3.5
Δ_{cs}

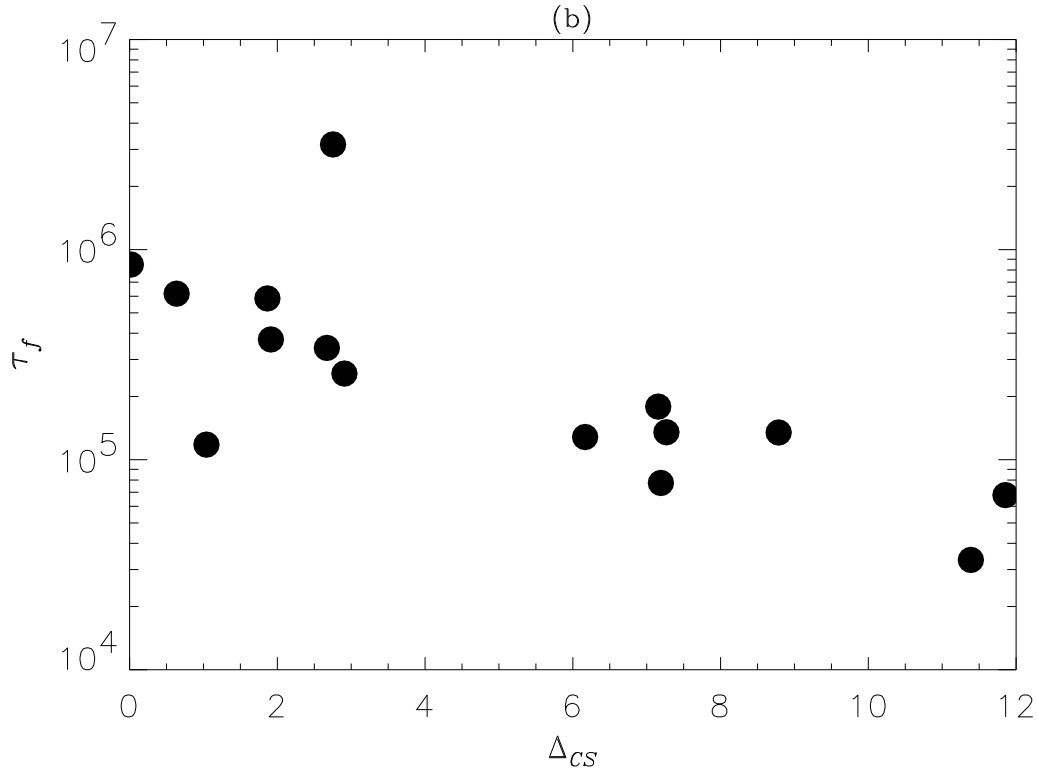
(b)
10^{7}
10^{6}
10^{5}
10^{4}
τ_f
0
2
4
6
8
10
12
Δ_{cs}

Fig. 22

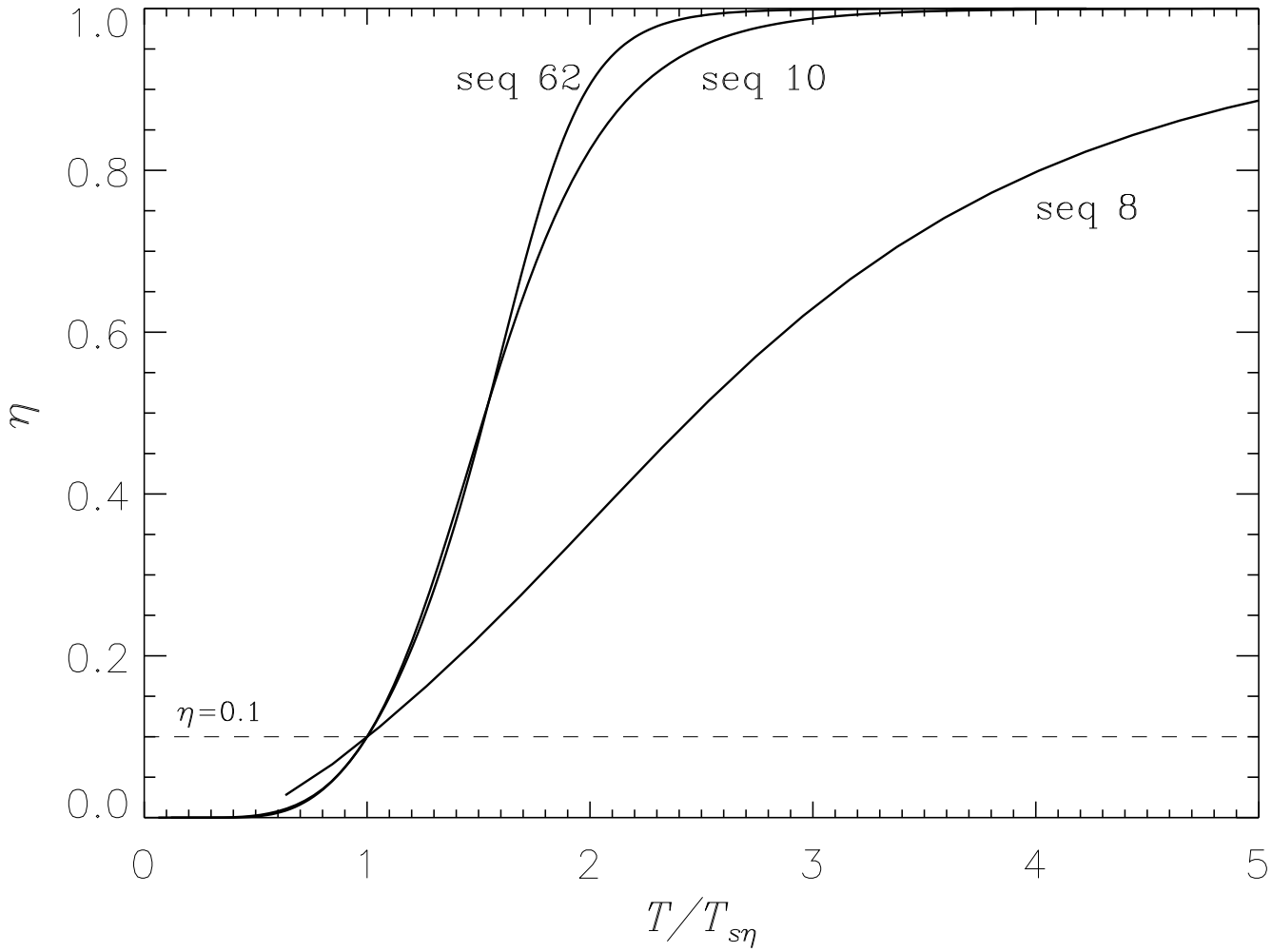

Fig. 23

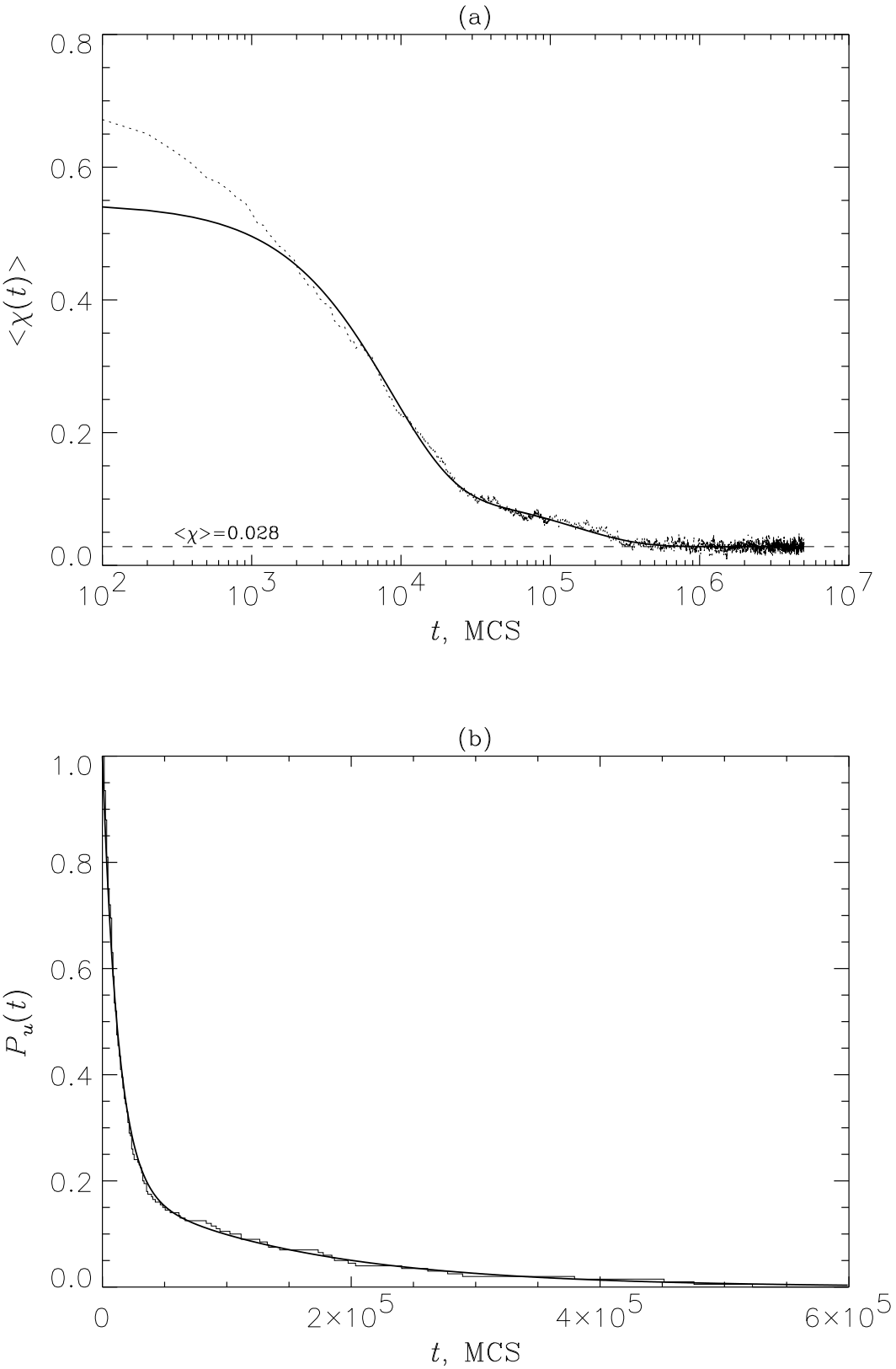
(a)
0.8
0.6
0.4
0.2
0.0
<χ(t)>
<χ>=0.028
10^2
10^3
10^4
10^5
10^6
10^7
t, MCS
(b)
1.0
0.8
0.6
0.4
0.2
0.0
P_u(t)
0
2×10^5
4×10^5
6×10^5
t, MCS

Fig. 24

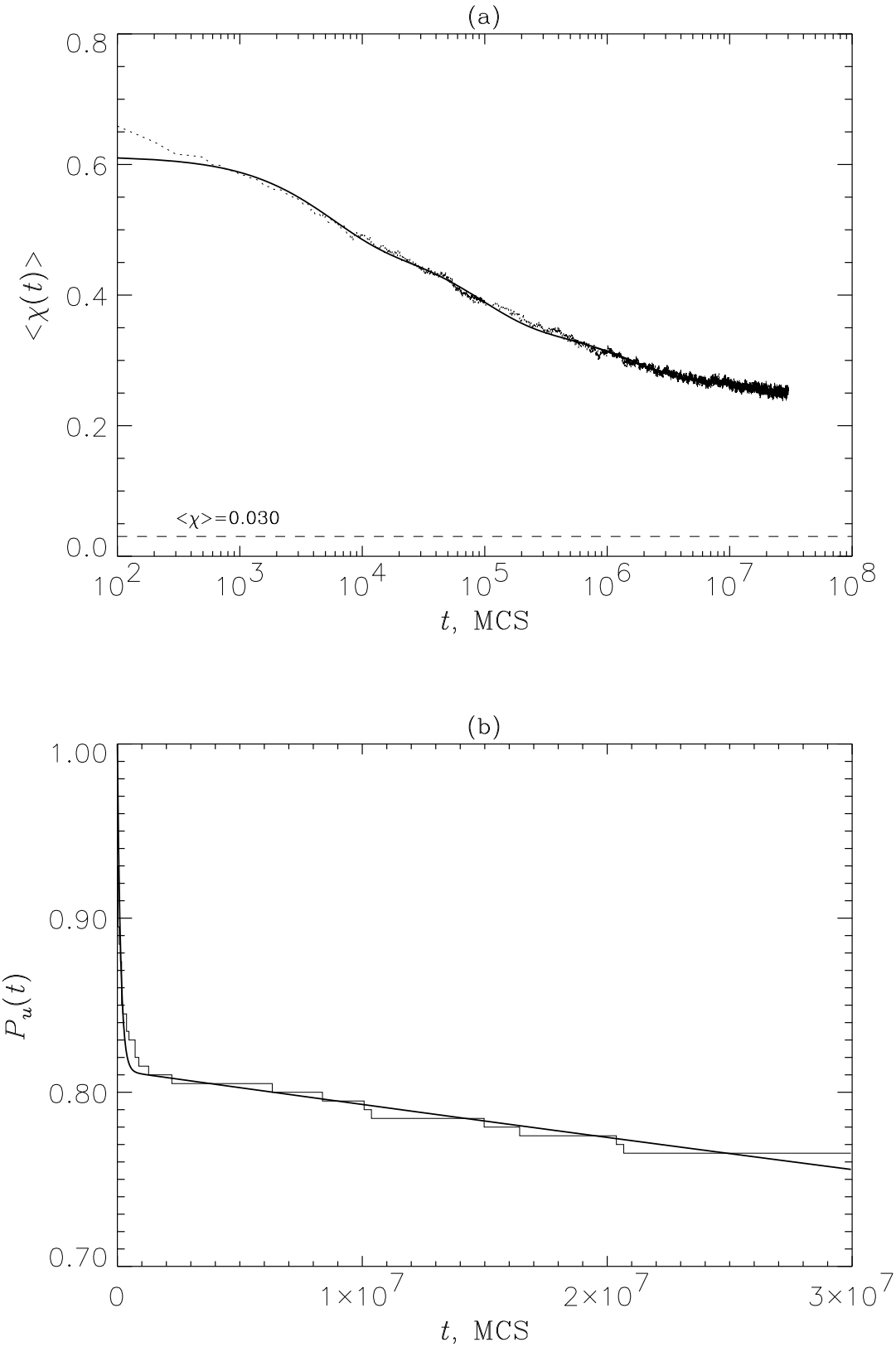
(a)
0.8
0.6
0.4
0.2
0.0
$<\chi(t)>$
<χ>=0.030
10^2
10^3
10^4
10^5
10^6
10^7
10^8
t, MCS
(b)
1.00
0.90
0.80
0.70
$P_u(t)$
0
1×10^7
2×10^7
3×10^7
t, MCS

Fig. 25

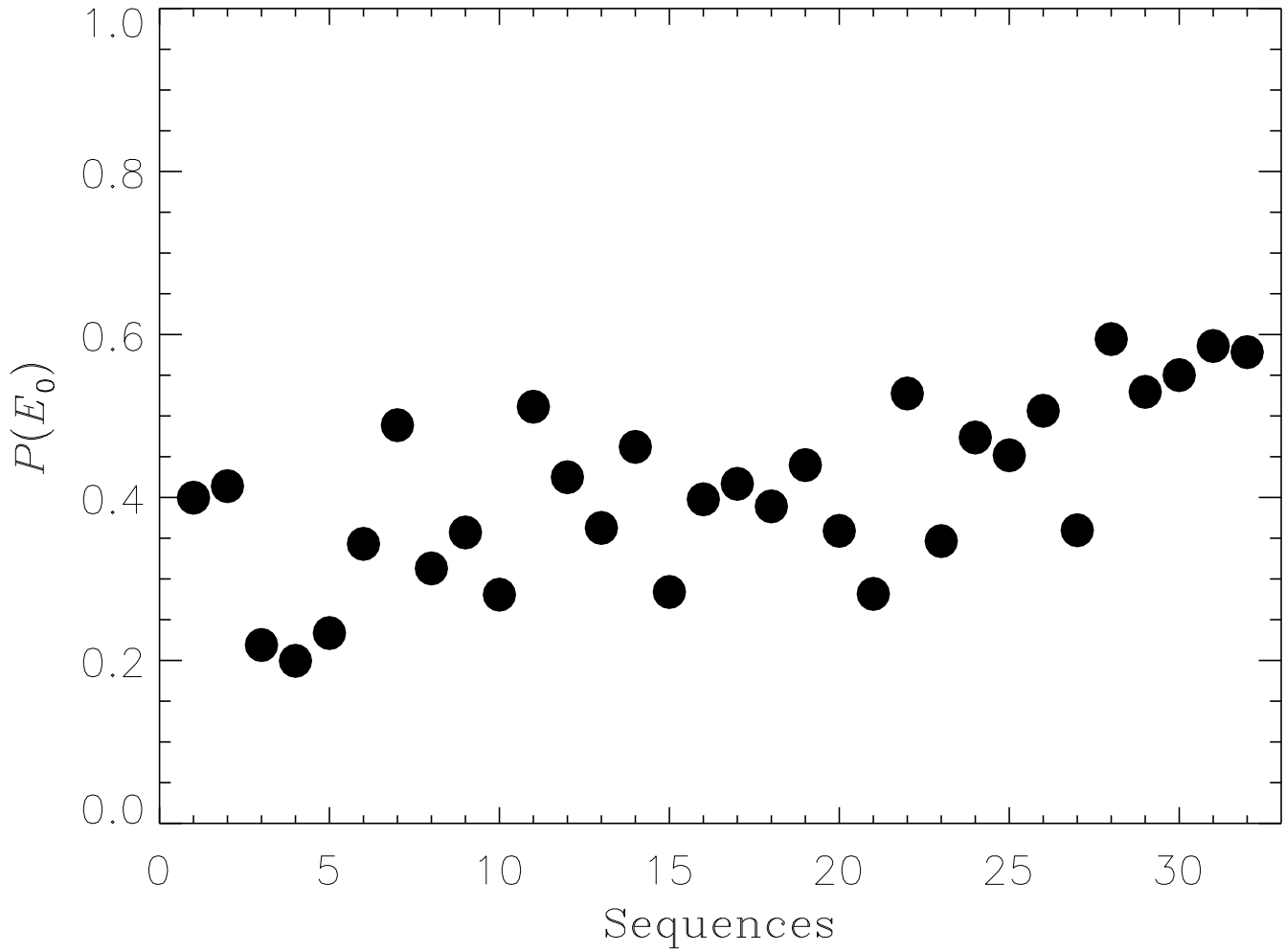

Fig. 26